

**ІНФОРМАЦІЙНІ ТЕХНОЛОГІЇ ТА СПЕЦІАЛЬНА БЕЗПЕКА
НАУКОВИЙ ЖУРНАЛ**

№ 1(008) 2022

ЗМІСТ

Musokhranov B.A.

COAL COKE BY BORIS MUSOKHRANOV.....2

Mudryk A., Kucherov O., Lavrovsky S.

UKRAINIUM STARTS THE D.I. MENDELEEV'S PERIODIC TABLE.....15

Kucherov O., Lavrovsky S.

VISIBLE ATOM.....29

РЕЦЕНЗІЇ ТА ІНФОРМАЦІЙНІ ПОВІДОМЛЕННЯ

ПРАВИЛА ДЛЯ АВТОРІВ63

Musokhranov B.A.

General director of the company OULIANA TRADING, S.L.

OULIANA TRADING, S.L., CALLE HELIODORO RODRIGUEZ GONZALEZ, 38005 SANTA CRUZ DE TENERIFE, SPAIN

COAL COKE BY BORIS MUSOKHRANOV

Annotation. The article presents a new allotrope of carbon - coal coke invented by Boris Musokhranov, which fundamentally differs from all known allotropes (both carbon and others) by the absence of hybrid bonds. These are unbound valence π - electrons; they are active and give Musokhranov's coke the maximum heat of combustion. The presence of four valence π -electrons is a condition for maximum coking, optimal quality with a minimum price. Consequently, the criterion for coking is the breaking of hybrid σ -bonds with their transformation into active π -electrons.

The article provides documents confirming copyright for Musokhranov's coal coke. It also lists companies and countries that violate these intellectual property rights.

Keywords. coke-chemical production; metallurgical coke; electron cloud densitometry; picoscope; Musokhranova's coal coke; heat of combustion; hybrid σ -bonds; active n - electrons.

Relevance of the topic. Coke-chemical production is the main direction of non-fuel use of hard coals in their technological processing by high-temperature carbonization into metallurgical coke for the production of iron and steel in the blast-furnace process.

The foundations of coke production were laid by D.I. Mendeleev, he wrote in 1899: "To increase the mass of metal in Russia, to reduce its cost, it would be very important that it was in the Urals that iron smelting on coke began." In the Donbas (1888), he expressed the idea of underground gasification of coal and returned repeatedly ("Combustible materials" - 1893, "Fundamentals of the factory industry" - 1897, "The Doctrine of Industry" - 1900— 1901).

During the transition period from a centrally planned economy to market methods of management, the existing raw coal base was destroyed, and by the beginning of the 21st century it was characterized by significant instability in terms of the grade composition of supplied coals and concentrates. The negative effect of the deterioration in the grade composition of coals was compensated by an increase in the level of "end-to-end management" of the quality of coal charges and coke and the technology of coke-chemical and blast-furnace production. At the same time, the preparation of coal charges for coking was evaluated on the basis of production experience data and indicators of the technical analysis of coals.

Formulation of the problem. The importance of the fuel industry of blast-furnace production is beyond doubt among specialists. Therefore, much attention has always been paid to the issues of prices and quality of coke, the main fuel agent of the blast-furnace process [1-3].

At the same time, world science and production had high achievements in the development of new highly efficient technologies for the production of coke and improving its quality. So, the following were tested: molded coke [4], coke from partially briquetted coal charge [5], and coke with

petroleum sintering additive (NPC) [6]. When selecting differentiated charge compositions, a problem arises that is attempted to be solved by mathematical modeling, taking into account the processes of heat transfer and thermal destruction of coal charge in coke ovens [7].

It is known that **lean coals** make the charge less shrinkage. Adding them to the charge reduces fracturing and increases the size of the coke. However, their **insufficient sintering** can lead to an increase in the attrition of coke, irregularity in the size of the pieces, and deterioration in the quality of the coke.

In addition, lean coals form a small amount of liquid phase, which is not enough to involve mixtures of grains of these coals in the sintering process. Therefore, in the charge of optimal sintering, so much liquid phase should be formed so that it is sufficient to wet the surface of the grains of the entire coked mass.

If there is little liquid phase, then the charge has a low caking capacity and is lean. If the mixture has excessive sintering (it is fatty), leaning components are added to it [8]. Those the maximum average of the components is possible to ensure the uniformity of the quality of the coal charge.

All fat-forming components of the coal charge have a large margin of sintering, which makes it possible to vary their content in the charge quite widely without worsening the sintering level [9].

Objective. The purpose of this work is to search for the optimal coke using picoscopy methods.

Main material. Carbon is the substance with the largest number of allotropic modifications. Picoscopic images were obtained for the following allotropic modifications of carbon: a) diamond [13]; b) graphite [12]; c) graphene [14]; d) nanotube [16]; e) rudenite [14]; f) destroys [13]. Picoscopic image is the electron cloud densitometry [12], which conveys the shape of all internal and valence electrons. The article [15] shows the impossibility of the existence of double covalent π -bonds.

In 1927, Geitler and London [17] carried out a quantum mechanical calculation of the hybridization of 1s molecular orbitals of the H₂ molecule. O.P. Kucherov [18] extended these quantum mechanical calculations to heavy atoms such as silicon. The success of this theory led to a series of studies in the field of chemical bonds and the creation by Pauling of the monograph "The Nature of Chemical Bonds" [19].

Further quantum mechanical calculations carried out by O.P. Kucherov [12] showed that the Pauli principle forbids twin hybridization. That is, there are no π -bonds, and, instead of them, there are unbound π -electrons. These electrons form elongated arms and create weak van der Waals forces.

Densitometry of electron clouds showed that the carbon atom in Musokhranov's coke does not have covalent strong σ -bonds. In this coke, four π -electrons weakly interact with the environment, are not bound but very aggressive, which causes its high heat transfer during combustion.

Direct visualization of valence electrons.

Direct visualization of valence electrons in the carbon atom of crystalline graphite was carried out by measuring the electron cloud density $p(x, y)$ using the electron beam shift effect (10 pm resolution).

Such measurements became possible thanks to a breakthrough in fundamental physics made by Ukrainian scientists A.P. Kucherov and S.E. Lavrovsky [20], namely the discovery of an unexpected natural phenomenon when an electron beam is displaced through a quantum superposition with an electron cloud. The result was a picoscope, a unique apparatus for direct visualization of pico-

dimensional objects: molecules, atoms, and chemical bonds.

The chemical element carbon has two internal and four valence electrons. Figure 1 shows a picoscopic image of crystalline graphite with an electron cloud density of carbon atoms $\rho(x, y)$. Internal electrons (pink spheres) form graphite planes. Strong σ -bonds sp^2 orbital green hybrids form covalent bonds in planes. π electrons (blue clouds) are pulled into the space between the graphite planes and connect the planes to each other.

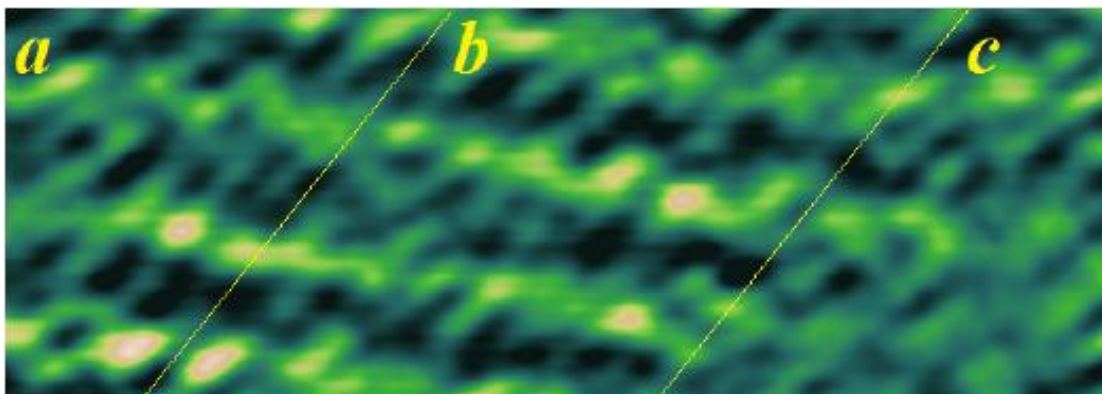


Fig.1. Phase transition from crystalline graphite to amorphous coke in the one picoscopic image: a) π -bonds reach out to neighboring atoms in the crystalline graphite; b) structure partially disappears and π -electrons don't reach the neighboring atoms; c), hybrid σ -bonds have disappeared and turned into π -electrons and create amorphous Musokhranov's coke.

Figure 1 on the right shows the picoscopic image of an electron cloud density of carbon atoms $\rho(x, y)$. Internal electrons (pink spheres) form graphite layers. Strong σ -bonds sp^2 orbital green hybrids form covalent bonds in layers. The π -electrons (blue clouds) are pulled into the space between the graphite layers and connect the planes to each other. The picoscopic image shows the process of the phase transition from crystalline graphite to amorphous coke. a) The π -bonds reach out to neighboring layers in the crystalline graphite. b) The structure partially disappears and π -electrons don't reach the neighboring layers. c) The hybrid σ -bonds have disappeared and turned into π -electrons. The crystalline structure has totally destroyed and the carbon atoms synthesize a new allotrope - amorphous Musokhranov's coke.

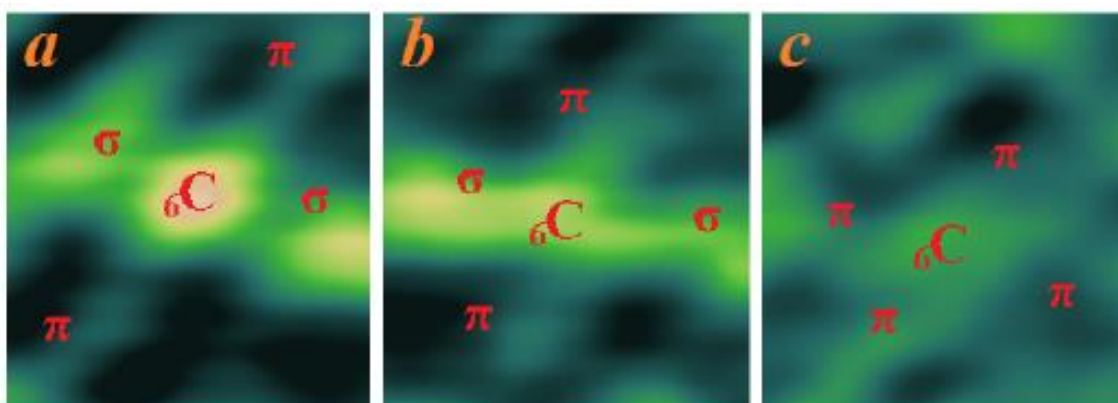


Fig.2. Picoscopic images of individual carbon atom in three different states: a) π - electrons reach out to neighboring layers in the crystalline graphite; b) structure partially disappears and π -electrons don't reach the neighboring layers; c), hybrid σ -bonds have disappeared, turned into π -electrons and create amorphous Musokhranov's coke.

By means of picoscopy, we traced the process of Musokhranov's coke synthesis at the super-level of one carbon atom. Figures 2 show the transition process of the carbon atom from crystalline to amorphous state. At all three figures the carbon atom has six electrons, that totally accordance to periodic table of D. I. Mendeleev. The first and second internal non-valence electrons form a pink sphere. The third and fourth valence electrons form strong σ bonds (green), which are sp^2 orbital hybrids. The fifth and sixth nonbonding π -electrons form blue clouds, which are attracting the neighboring layers. The space around the atom is mostly black because the density of the electron cloud in the space between atoms is zero. a) The π -bonds reach out to neighboring layers in the crystalline graphite. b) The structure partially disappears and π -electrons don't reach the neighboring layers. c) The hybrid σ - bonds have disappeared and turned into π -electrons. The crystalline structure has totally destroyed and the carbon atoms synthesize a new allotrope - amorphous Musokhranov's coke.

Coke is an allotrope of carbon with zero hybridization, in other words, it is a substance in which strong hybrid σ -bonds are completely absent and each carbon atom has four disconnected n -electrons.

Consequently, all coals are coking, but each brand of coal needs its own coking technology. Therefore, the criterion for coking is the breaking of hybrid σ -bonds with their transformation into active n -electrons [15].

Production technology. Taking into account the realities of the new stage, it became possible to develop scientific and technical foundations for the formation of a raw material base for coking using visual control of the selection of optimal components of coal charges to produce high-quality metallurgical coke under conditions of instability of the grade composition and characteristics of the initial coals. In accordance with this, the problem of developing a criterion for obtaining Musokhranov coal coke was formulated and solved [11].

The formation of the optimal quality of coke for the entire range of indicators is achieved by computer selection of the composition of coal charges and optimization of the conditions for their coking by picoscopy visualization.

Since complex indicators obey the rule of additivity in mixtures, they are used in the development of differentiated mixture compositions with specified Ro and FSI indicators.

The picoscopy visualization allows the selection of charge compositions by optimizing the ratio of free swelling index - FSI (or the thickness of the plastic layer - Y) and the reflectivity of vitrinite Ro (or the yield of volatile substances - V). The result is Musokhranov's coal coke.

If sintering (fatty) components prevail in the charge, then a large amount of liquidmoving products is formed, and they have a low viscosity (FSI is 6-8 units, Ro is 0.8-1.1%). In this case, the coke will be highly expanded, highly reactive, with large pores and low mechanical strength. If poorly sintering (leaning) components prevail in the charge (FSI is 14 units, Ro is 1.20-2.00%), then the coke will turn out to be slightly expanded with very small pores. Such coke has low mechanical strength and very low reactivity.

To ensure optimal volume and viscosity values for fluid products, it is necessary that the FSI of the coal mixture sent for coking range from 5 units to 5 units. (the thickness of the plastic layer was $Y=17$ mm), the reflectivity of vitrinite should be 1.15% -1.2% (volatility of about 30%). These parameters are typical for high-quality grade K coals, which can produce good coke without additives. However, the resources of these coals are already very small. In order for the coal mixture to have quality parameters close to grade K, it is necessary to include several sintering and lean coals in it. To simplify the mixture preparation technology, it is advisable to pre-prepare two groups of components - well-caking (fat, that is, rich in coal grades Zh, GZh, K, KZh) and low caking (lean, that is, rich in coal grades KO, SS, OS, TS).

Oily components must have an FSI index of at least 5 (plastic layer thickness over 15 mm) and a Ro value of up to 1.15%. The lean components must have an FSI index of up to 4 1/2 (plastic layer thickness up to 14 mm) and a Ro value of more than 1.15%. When mixing components with such properties with each other or with individual coals, mixtures with optimal characteristics are obtained.

Charges for coking can be composed of two compositions - fat and lean, or from several components, including a fat composition and individual lean coals or a lean composition and individual fat-laden coals. The limits of the content of fatty components in batches can be from 20 to 80%, lean components can be contained from 5 to 70% by weight of the batch.

In the proposed compositions, the content of components varies from 3 to 97% wt. depending on which the content of lean components also varies.

The first charge is more suitable for narrow-chamber coke oven batteries, the second - for wide-chamber batteries. Grades of coal are given in accordance with "GOST 25543-88 hard coal" [10]. Concentrate grades: K, KZh, Zh, GZh are similar in their characteristics to HCC coals - hard coking coal according to the international classification, concentrate grades: GZhO, KO, KS, OS are similar in their characteristics to SSCC coals - weakly caking coking coal according to the international classification. Coals of grades: KSN, TS, SS, G are similar to energy coals Thermal Coal / Steam Coal coals according to the international classification. These circumstances make it possible to obtain high-quality charge, using coals of two classifications to obtain metallurgical coke of high mechanical strength. Industrial production of coal coke of Boris Musokhranov will be shown in the next section.

Precedent is an exclusive right.

<p>ЛИЦЕНЗИОННЫЙ ДОГОВОР № 31.12.27 26 июля 2022 г. Санта Круз де Тенерифе, Испания OULIANA TRADING, S.L., рег. № B38667572, адрес: SPAIN, SANTA CRUZ DE TENERIFE, S.C.TENERIFE, 38005, C\ HELIODORO RODRIGUEZ GONZALEZ, 1A P.4, 3 IZQ, именуемое в дальнейшем "Лицензиар", в лице Генерального директора Бориса Мусохранова, действующего на основании Устава, с одной стороны, И SOBELA TRADING COMPANY, INC, рег. № 4314848, адрес: 8861 195 PLACE, HOLLIS, NY, 11423, United States of America, именуемое в дальнейшем "Лицензиат", в лице директора София Бернард, действующая на основании Устава, с другой стороны,</p> <p>а вместе именуемые Стороны, принимая во внимание, что:</p> <ul style="list-style-type: none"> -Лицензиар является патентообладателем: -патента № RU2448146, зарегистрирован в международной системе PCT № ES2007/000199, 10 апреля 2007 года, публикация в WIPO 2008/122678, 16 октября 2008 года; зарегистрирован в Государственном реестре патентов Российской Федерации, 20 апреля 2012 года, бюллетень № 11 «Шихта для получения металлургического кокса (варианты)»; -патента № UA92783, зарегистрирован в международной системе PCT № ES2007/000199, 10 апреля 2007 года; зарегистрирован в Государственном реестре патентов Украины, 10 декабря 2010 года, «Шихта для получения металлургического кокса (варианты)»; - Также, выдано Авторское свидетельство № 00/2019/3425, выданное Центральным реестром интеллектуальной собственности, 7 августа 2019 года, г. Мадрид, Королевство Испании; на публикации запатентованных технологий в научном журнале «Информационные технологии и Специальная безопасность»; <p>Все вышеперечисленное является интеллектуальной собственностью Лицензиара, далее именуемое как «Товар».</p> <ul style="list-style-type: none"> - Лицензиат желает приобрести, на условиях настоящего Договора, в рамках неисключительного права, неисключительную Лицензию на применение интеллектуальной собственности Лицензиара в гражданском 	<p>LICENSE CONTRACT № 31.12.27 26th of July, 2022 Santa Cruz de Tenerife, Spain OULIANA TRADING, S.L., reg. no. B38667572, address: SPAIN, SANTA CRUZ DE TENERIFE, S.C.TENERIFE, 38005, C\ HELIODORO RODRIGUEZ GONZALEZ, 1A P.4, 3 IZQA, on behalf of the general director Boris Musokhranov acting on the basis of Statutes, named further "Licensor", on the one hand And SOBELA TRADING COMPANY, INC, reg. no. 4314848, address: 8861 195 PLACE, HOLLIS, NY, 11423, United States of America, on behalf of director Sofia Bernard acting on the basis of Statutes, named further "Licensee", on the other hand,</p> <p>both further named "Parties", in view of that:</p> <ul style="list-style-type: none"> -The Licensor is the patent holder of: <ul style="list-style-type: none"> - patent No. RU2448146, registered in international system PCT No. ES2007/000199, 10th of April, 2007, published in WIPO 2008/122678, 16th of October, 2008; registered in State registry of patents of Russian Federation, 20th of April, 2012, bulletin No.11 "Mixture of minerals and fluxes for obtaining metallurgical coke (variants)"; - patent UA92783, registered in international system PCT No. ES2007/000199, 10th of April, 2007, registered in State registry of patents of Ukraine, 10th of December, 2010, "Mixture of minerals and fluxes for obtaining metallurgical coke (variants)"; - Also, the Certificate of Authorship No. 00/2019/3425 was issued by Central registry of intellectual property, 7th of August, 2019, Madrid, Kingdom of Spain; for publications of patented technologies in the scientific journal "Information technologies and Special security"; All the above stated are the intellectual property of the Licensor, hereinafter referred to as the "Commodity" -The Licensee wishes to acquire, under the terms of this Contract, within a non-exclusive right, a non-exclusive License for the use of the Licensor's intellectual property in civil circulation, in order to: manufacture, use in circulation, store for these purposes a product made on
--	---

<p>обороте, в целях: изготовления, применения в обороте, хранения для этих целей продукта, изготовленного на основе вышеуказанной интеллектуальной собственности; а также, право на применение в гражданском обороте коксующихся и пригодных для слоевого коксования марок углей, указанных в статье «Изобретение с применением компьютерной подборки дифференцированных композиций шихт для получения металлургического кокса максимального качества», раздел - Право на применение изобретения.</p> <p>Заклучили настоящий Договор о следующем:</p> <p>1.ПРЕДМЕТ ДОГОВОРА.</p> <p>1.1. Лицензиар предоставляет Лицензиату, на условиях данного Договора, неисключительную Лицензию на весь пакет (товар) интеллектуальной собственности Лицензиара, а именно: патент № RU2448146, патент № UA92783, авторское свидетельство N2 00/2019/3425, статья с технологией ИЗОБРЕТЕНИЕ С ПРИМЕНЕНИЕМ КОМПЬЮТЕРНОЙ ПОДБОРКИ ДИФФЕРЕНЦИРОВАННЫХ КОМПОЗИЦИЙ ШИХТ ДЛЯ ПОЛУЧЕНИЯ МЕТАЛЛУРГИЧЕСКОГО КОКСА МАКСИМАЛЬНОГО КАЧЕСТВА; на все формулы, указанные в патентах и статье; все варианты, указанные в таблицах перечисленных документов на применение в гражданском обороте, Закон права первой руки и применение в обороте коксующихся и пригодных для коксования марок углей: Ж (жирные), ГЖ (газовожирные), ГЖО (газово-жирные отощённые), КЖ (коксовые жирные), К (коксовые), КО (коксовые отощённые), спекающиеся), ОС (слабоспекающиеся), низкометаморфизованные), производства двухкомпонентной шихты в пределах от 3% до 97% и композиции таких смесей, предназначенные для коксования, а также в энергетических секторах.</p> <p>1.2. Право на использование предмета настоящего Договора, предоставляется Лицензиату совместно с Лицензиаром на территориях стран Содружества Независимых Государств (СНГ), Украины, Монголии, Китая, Индонезии, стран Евросоюза, США, Индии и в любых других государствах, где могут использоваться вышеперечисленные технологии с указанными марками углей: концентрат марок К, КЖ, Ж, ГЖ по своим характеристикам аналогичны НСС - твёрдый</p>	<p>the basis of the above stated intellectual property; and also, the right to use in civil circulation of coking and suitable for layered coking coal grades specified in the article "The invention with the application of a computer selection of differentiated compositions of mixtures for producing metallurgical coke of maximum quality", section - Right to apply the invention.</p> <p>have agreed as follows:</p> <p>1. THE SUBJECT OF THE CONTRACT.</p> <p>1.1.The Licensor grants to the Licensee, under the terms of this Agreement, a non-exclusive License for the entire package (goods) of the Licensor's intellectual property, namely: patent No. RU2448146, patent No. UA92783, Authorship certificate No. 00/2019/3425, article with technology THE INVENTION WITH THE APPLICATION OF A COMPUTER SELECTION OF DIFFERENTIATED COMPOSITIONS OF MIXTURES FOR PRODUCING METALLURGICAL COKE OF MAXIMUM QUALITY; on all formulas specified in patents and article; all variants indicated in the tables of the listed documents for use in civil turnover, the Law of the First Hand and the use in turnover of coking and suitable for coking grades of coal: Zh (fat), GZh (gas fat), GZhO (gas fat semi-lean), KZh (coke fat), K (coke), KO (coke semi-lean), TS (lean caking), OS (semi-lean caking), SS (weakly caking), G (gas), KS (coke weakly caking), KSN (coke weakly caking low metamorphic coal), and coal blends for the production of a two-component charge in the range from 3% to 97% and the composition of such blends intended for coking, as well as in the energy sectors.</p> <p>1.2.The right to use the subject of this Contract is granted to the Licensee jointly with the Licensor in the territories of the Commonwealth of Independent States (CIS), Ukraine, Mongolia, China, Indonesia, EU countries, the USA, India and in any other states where the above technologies with the indicated coal grades can be used: concentrate grades K, KZh, Zh, GZh are similar in characteristics to HCC - hard</p>
--	---

<p>коксующийся уголь; концентрат марок ГЖО, КО, КС, ОС по своим характеристикам аналогичны SSCC - слабоспекающийся коксующийся уголь, PCI - размельчённый уголь для впрыска; марки углей КСН, ТС, СС, Г по своим характеристикам аналогичны Thermal Coal/Steam Coal - энергетические угли, после выполнения всех условий, указанных в пп. 7.1 и 7.2 настоящего Договора.</p>	<p>coking coal; concentrate grades GZhO, KO, KS, OS are similar in characteristics to SSCC - semi-soft coking coal, PCI - Pulverised Coal for injection; coal grades KSN, TS, SS, G are similar in characteristics to Thermal Coal/Steam Coal; after meeting all the conditions specified in clauses 7.1 and 7.2 of this Contract</p>
---	--

In the section Precedent - as an exclusive Right, it is indicated that a non-exclusive license for the entire package of intellectual property (goods) of Ouliana Trading, S.L., namely: patent No. RU2448146, patent No. UA92783, authorship certificate No. 00/2019/3425, article [11] was acquired by the American company SOBELA TRADING COMPANY, INC, reg. No 4314848 and currently no company have such rights. Given the fact that there are no other coking coals in nature, the products of other companies produced without the permission of the copyright holder become counterfeit, according to the Law - it is a crime. On the basis of legislative acts to combat counterfeiting and falsification, the Prosecutor's Office is obliged to arrest criminal products and means of production within three days. Further in the text, lists of patent and copyright infringing companies.

LIST OF INFRINGING COMPANIES, RUSSIA

1. OJSC MMK Group, owner Viktor Rashnikov

- PJSC Magnitogorsk Iron & Steel Works
- LCC MMK-UGOL (CPP Belovskaya)
- LCC MMK-LMZ
- JSC MMK-METIZ
- CJSC INTERKOS-IV
- MMK Metalurji Sanayi, Ticaret ve Liman Isletmeciligi A. S.

2. EVRAZ HOLDING, owners Roman Abramovich / Aleksandr Abramov

- CPP Abashevskaya
- CPP Kuznetskaya
- JSC Joint Coal Company Yuzhkuzbassugol (CPP Raspadskaya)
- JSC EVRAZ ZSMK (CPP ZSMK)
- JSC EVRAZ NTMK
- JSC Novokuznetsk Iron & Steel Works
- Coal Company Mezhegeyugol

- 3. OJSC KOKS (Kemerovokoks) owner Evgeniy Zubitskiy**
 - CPP Berezovskaya

- 4. Coal Company Kuzbassrazrezugol, owners Iskander Makhmudov / Andrey Bokarev**
 - CPP Vakhrushevskaya
 - CPP Kedrovskaya
 - CPP Bachatskaya-Energeticheskaya
 - CPP Bachatskaya-Koksovaya
 - CPP Krasnobrodskaya-Koksovaya
 - CPP Kaltanskaya- Energeticheskaya

- 5. OJSC Mechel Group, owner Igor Zyuzin**
 - LCC UK Mechel-Mining (OJSC Yuzhniy Kuzbass, Yakutugol Holding Company, Mining processing plant Korshunovskiy, JSC Moscow coke and gas plant, Mechel-Koks)
 - LCC UK Mechel-Stal (OJSC Chelyabinsk Iron & Steel Works, JSC Beloretskiy Iron & Steel Works, OJSC Izhstal, OJSC Uralskaya kuznitsa, JSC Vyartsilya Metal Products Plant, CJSC Mechel Nemunas, LCC Bratsk Ferroalloy Plant, OJSC Southern Urals Nickel Plant)

- 6. OJSC NLMK Group, owner Vladimir Lisin**
 - Novolipetsk Iron & Steel Works
 - Mining processing plant Stoilenskiy
 - Altai-Koks

- 7. OJSC Severstal Group, owner Aleksey Mordashov**
 - Cherepovetsk Iron & Steel Works
 - Izhora Pipe Plant
 - Vorkutaugol
 - Severstal-Metiz
 - Mining processing plant Yakovlevskiy

- 8. OJSC Gazprom, owner State of the Russian Federation**

- 9. JSC Rosoboronexport, owner State of the Russian Federation**

- 10. Metalloinvest, owner Alisher Usmanov**

- 11. Kolmar, owner Anna Tsivileva**

LIST OF INFRINGING COMPANIES, KAZAKHSTAN

1. Bogatyr Komir (Joint venture RUSAL (**Oleg Deripaska**) and Kazakhstan holding Samruk-Kazyn)
2. Karaganda Iron & Steel Works
3. ArcelorMittal Temirtau
4. Aktobe ferroalloy plant
5. Aksu Ferroalloy Plant

LIST OF INFRINGING COMPANIES, UKRAINE

1. Metinvest Group, owner **Rinat Akhmetov**
 - Avdiivka Coke Plant
 - Dneprovsky Coke Plant
 - Donetskstal Iron & Steel Works
 - Enakievo Coke Plant
 - Enakievo Iron & Steel Works
 - Zaporiyiakoks
 - Zaporiyiastal
 - Mining processing plant Ingulets
 - Krivoy Rog iron ore plant
 - Azovstal Iron & Steel Works
 - Mariupol Iron & Steel Works
 - Mining processing plant Severniy
 - Khartsyzsk Pipe Plant
 - Mining processing plant Tsentralniy
 - Yuzhkoks
 - LCC Unisteel
 - Mining processing plant Yuzhniy
2. Interpipe, owner **Viktor Pinchuk**
 - Interpipe NIKO TUBE
 - Interpipe NMTZ
 - Interpipe Steel
 - Nizhnedneprovsk Pipe Rolling Plant
3. Ferrexpo, owners **K. Zhevago (51%), BXR Group Limited (25%)**
 - Mining processing plant Belanovskiy
 - Mining processing plant Eristovskiy

- Mining processing plant Poltavskiy
- 4. Donbass Industrial Union, owners **EVRAZ (50,1%), Sergey Taruta and Oleg Mkrtchan (49,9%)****
 - Alchevsk Iron & Steel Works
 - Dnepr Iron & Steel Works
 - Dnepropetrovsk Pipe Plant
- 5. ArcelorMittal Group**
 - ArcelorMittal Krivoy Rog
- 6. Donetskstal Group**
 - Yasinovskiy Coke Plant
 - Makeevkoks
- 7. DCH Group, owner **Oleksandr Yaroslavsky****
 - Dneprovskiy Iron & Steel Works
 - Sukhaya Balka
- 8. Privat Group, owners **Gennady Bogolyubov, Igor Kolomoisky, Alexey Martynov****
 - DMZ Kominmet
 - Dneprospetsstal
 - Zaporozhye Ferroalloy Plant
 - Mining processing plant Marganets
 - Mining processing plant Pokrov
 - Nikopol Ferroalloy Plant
 - Stakhanovskiy Ferroalloy Plant
- 9. CPP Chervonogradskaya**
- 10. State company Lvovugol**

Conclusion

Scientific developments, technologies, intellectual property rights are crucial in the development of any society. The OULIANA TRADING, S.L. company repeatedly applied to the European Commission and the European Parliament so that internal investigations were carried out on the gas transmission projects: Turkish Stream, Nord Stream, Nord Stream 2 and Power of Siberia. Based on these facts the company has stated that large-diameter pipes used by PJSC Gazprom are counterfeit and falsified due to the fact that they are made of metal using Spanish technology without the permission of the copyright holder, and, in fact, are criminal projects. The leadership of the European

Commission ignored our appeals, although the Berne Convention on Copyright was ratified by 167 states, including the countries of the European Union. Disregard for legislative acts led to disastrous results. The requirements of the Spanish company Ouliana Trading, S.L. remain the same: replace counterfeit large-diameter pipes with similar ones made from licensed metal in all four projects. To prove that the metal is falsified, it is enough to check: 1- commodity-transport and railway waybills, where the marking of the cargo is mandatory; 2- documentation from coal preparation shops; 3 - documents of processing plants, which indicate the proportions for mixing coal grades when obtaining a graded concentrate; 4-coal site metcoal.ru, where you can trace the movement of all coals.

This year, President of the Russian Federation V. Putin signed the Federal Law of March 26, 2022 No. №74-FZ “On Amendments to Certain Legislative Acts of the Russian Federation”, and freed individuals and companies from criminal prosecution for committing unlawful acts, thus the President of the Russian Federation V. Putin, de jure and de facto, approved the Russian Federation as a criminal state. Consequently, all products produced in a criminal state, initially, become criminal. Companies from the United States, the European Union, India, China, Great Britain, Turkey and other countries need to pay attention to the fact that when cooperating with Russian companies, they become accomplices in the criminal business. Such actions are prosecuted under the national laws of all countries, as well as under the norms of international law. The governments of these and other countries need to stop illegal actions by law. Otherwise, inaction and concealment are regarded as malfeasance.

Literature

1. Syskov K.I. Theoretical foundations for assessing and improving the quality of blastfurnace coke. - M.: Metallurgy, 1984. - 182 p.
2. Dzhigota A.D., Kostenko G.S., Kovalenko P.L. Characteristics of the quality of coke of some metallurgical enterprises // Issues of iron production in blast furnaces. Sat.tr. CHM - M.: Metallurgy, 1984. - P. 64-72.
3. Rudyka V.I. The role and importance of the technological base at the current stage of development of metallurgical and coke production. // Coal chemical journal. - 2006. - No. 5, 6. - P.3-8.
4. Investigation of the quality of the return batch of molded coke / Yu.B. Tyutyunnikov, L.G. Sintserova, V.V. Gavrikov et al. // Coke and Chemistry. -1974. - No. 6. - P.13-18.
5. Dyukanov A.G., Kaftan Yu.S., Biryukov Yu.V. et al. Influence of grade composition of briquetted coal blends on coke strength // Coke and Chemistry. - 1983. - No. 1. - P.6-7.
6. The role of mesogenic additives in the formation of coke structure / E.M. Tait, A.I. Olfert, G.I. Yenik et al. // Coke and Chemistry. - 1984. - No. 12. - P. 22-25.
7. Gyulmaliev A.M., Gagarin S.G., Trifonov V.N. Mathematical modeling of heat transfer and thermal destruction of coal charge in coke ovens// Coke and Chemistry. 2004. No. 9. S. 15-26.
8. Leibovich R.E. "Technology of coke production" - M., 1992, p. 55.
9. Kaftana Yu.S. etc. "Development of differential compositions for coke oven batteries with furnace chambers of different volumes" - J.NN. "Coke and Chemistry", 1990, p.11.
10. Musokhranov B.A. «Problems of copyright protection in the example of invention in

coke-chemical industry» / «Information technology and special security» (2018)

(<http://science-ua.com/gallery/maketrn2-1.pdf#page=2>)

11. B.A. Musokhranov, The invention with the application of a computer selection of differentiated compositions of mixtures for producing metallurgical coke of maximum quality. Information technology and special security (2020), 4-15

(<http://science.ua.com/gallery/maketrn6.pdf#page=4>)

12. Kuchеров O., Electron Cloud Densitometry of Inner and Valence Electrons in Carbon Allotropes/ Applied Functional Materials (AFM) 2022/03, Vol.2, Iss.1, 36-43

(<https://doi.org/10.35745/afm2022v02.01.0002>)

13. Kuchеров O., Rud A., Gubanov V., Biliy M. Spatial 3d Direct Visualization of Atoms, Molecules and Chemical Bonds // American Journal of Applied Chemistry. — 2020. — T. 8, № 4. — С. 94—99. DOI: (<https://doi.org/10.11648/j.ajac.20200804.11>)

14. O. P Kuchеров & A. D. Rud (2018) Direct visualization of individual molecules in molecular crystals by electron cloud densitometry, Molecular Crystals and Liquid Crystals, 674: 1, 40-47. (<https://DOI:10.1080/15421406.2019.1578510>)

15. Kuchеров O. P. "Direct Visualization of Active Valence Electrons in Carbon Allotropes". American Journal of Engineering Research (AJER), vol. 11(02), 2022, pp. 1925.

MATERIALSE (NANO-2017)

Chernivtsi.

(<https://www.ajer.org/papers/Vol-11-issue-2/D11021925.pdf>)

16. O.P. Kuchеров, S.E. Lavrovsky, Electron Trajectory Shifting Effect. Abstract book. International research and practice conference: NANOTECHNOLOGY AND NANO- (<http://www.iop.kiev.ua/~nano2017/files/abstracts/Kuchеров.pdf>)

17. Heitler, W.& London, F. "Wechselwirkung neutraler Atome und homopolare Bindung nach der Quantenmechanik" [Interaction of neutral atoms and homeopolar bonds according to quantum mechanics]. Zeitschrift fur Physik. 15-Humphrey, W.; Dalke, A.; Schulten, K. "VMD - Visual Molecular Dynamics" J. Molec. Graphics, 1996 14(1), 33-38.

18. Kuchеров, O. P "Direct Visualization of Covalent Chemical Bonds in Crystalline Silicon". American Journal of Engineering Research (AJER). 2021, 10(6): 54-58. (<https://www.ajer.org/papers/Vol-10-issue-6/G10065458.pdf>)

19. Pauling, L. (1960). The Nature of the Chemical Bond. Cornell University Press. pp. 340-354.

20. O.P. Kuchеров, S.E. Lavrovsky, Picoscopy - the Direct Visualization of Molecules. Information technology and special security (2016), 12-41

(<http://science-ua.com/gallery/maketrn2-1.pdf#page=12>)

Mudryk Andrey
Kucherov Olexandr
Lavrovsky Sergey

UKRAINIUM STARTS THE D.I. MENDELEEV'S PERIODIC TABLE

Company "GIGAHARD" ltd.
EUROPE, Bulgaria, Plovdiv 4000, EU Herbos Business Center office 105
Site: picoscopy.com
E-mail: info@picoscopy.com

Abstract. The paper presents further studies of the ukrainium which is a chemical element of the D.I. Mendeleev's periodic table. As a result, it was possible to finish the building the periodic table D.I. Mendeleev. The ukrainium has been shown to create hurricane eyewalls and clouds in Earth's atmosphere. Picoscopy methods made it possible to see the ukrainium atoms in the pentane molecule.

Keywords: D.I. Mendeleev's periodic table; ukrainium; picoscopy.

Мудрик Андрій
Кучеров Олександр
Лавровський Сергій

ПЕРІОДИЧНА СИСТЕМА Д.І. МЕНДЕЛЄЄВА ПОЧИНАЄТЬСЯ З УКРАЇНІЯ

Анотація. У статті представлені подальші дослідження українію, який є хімічним елементом періодичної системи Д.І. Менделєєва. В результаті вдалося закінчити будівництво періодичної системи Д.І. Менделєєва. Доведено, що україній створює стіну ока урагану та хмари в атмосфері Землі. Методи пікоскопії дозволили побачити атоми українію в молекулі пентану.

Ключові слова: Д.І. Періодична система Менделєєва; україній; пікоскопія.

INTRODUCTION

The ukrainium *Ua* is the chemical element of the periodic table D.I. Mendeleev number zero [1]. It occupies a cell in the first row of a zero group, it precedes hydrogen with number one, has number zero and makes the periodic table complete. This element is stable, in its natural form it is widely found both on Earth and in space [2].

The ukrainium starts the D.I. Mendeleev's table. Ukrainium *Ua* is in the D.I. Mendeleev's periodic table of chemical elements.

The atomic weight of this material is less than hydrogen; hence it is an element of the D.I. Mendeleev's periodic table with the number zero.

This material is a new chemical element which has its own place in the periodic table of Mendeleev: in the first period of group zero, see Fig. 1.

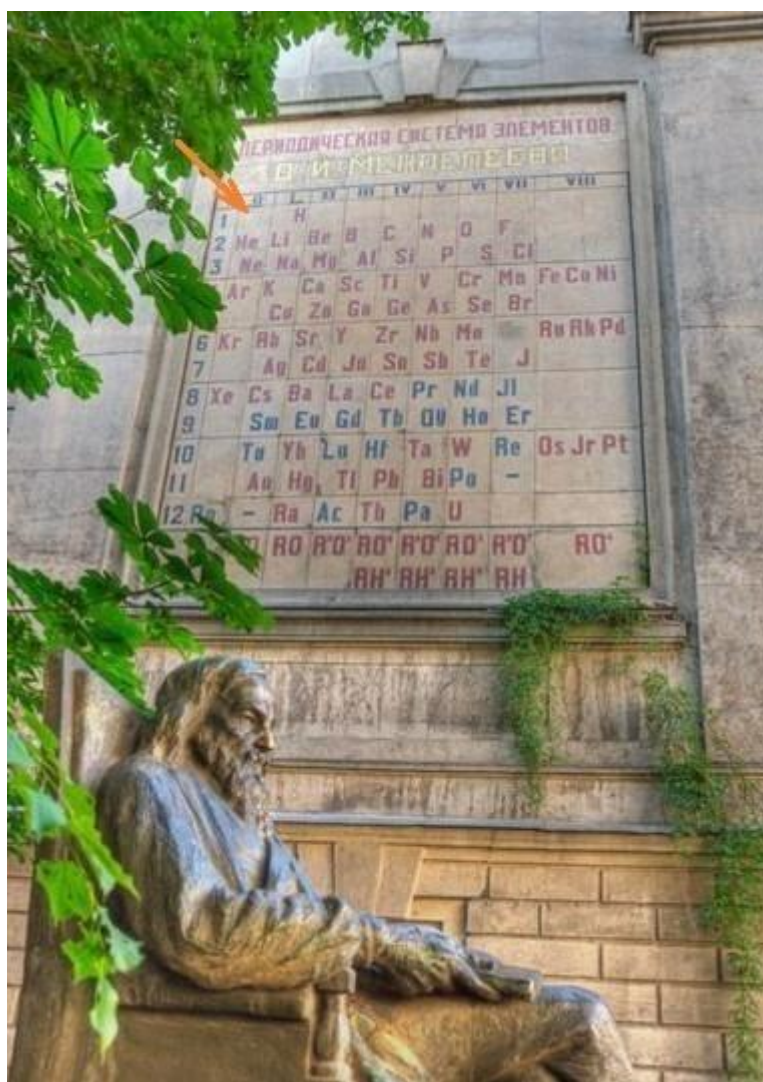


Fig.1. Monument to D.I. Mendeleev. All-Russian Research Institute of Metrology named after D.I. Mendeleev. St.-Petersburg.

In “An attempt at a chemical understanding of the world ether” (1902), D. I. Mendeleev considers an unknown inert gas with an atomic mass equal to one, giving it a place in the zero group before hydrogen. According to Mendeleev, this element must be found in the Earth’s atmosphere, as shown by the arrow in Figure 1.

For a long time, it was thought that an element with the number zero, like helium, was found in the Sun, namely in the solar corona. This was indicated by a band of intense radiation in the green region of the spectrum, which did not belong to any known element. It was given the name coronium.

However, coronium did not survive long in the scientific and academic literature. In 1939 astrophysicists Bengt Edlen and Walter Grotrian proved that the spectral line of 530.3 nm belongs to highly ionised iron (Fe¹³⁺).

The ukrainium finishes the Mudryk electron table formation. This is a new chemical element, which has its place in the periodic table of D.I. Mendeleev in the first period of the zero group. Its valence is zero, as in noble gases.

Ukrainium Ua, the zero element of the first period, finally fills the initial cell of the periodic table of chemical elements by D.I. Mendeleev, as a result of which the periodic table gets its completed form, Figure2.

↓Period	Group →	0	1	2	8	9	10	11	12	13	14	15	16	17	3	4	5	6	7	
1 = 1s 2×1 = 2 elements		Ua	H																	
2 = 2s 2p 2×(1+3) = 8 elements		He	Li	Be											B	C	N	O	F	
3 = 3s 3p 2×(1+3) = 8 elements		Ne	Na	Mg											Al	Si	P	S	Cl	
4 = 4s 4d 4p 2×(1+3+5) = 18 elements		Ar	K	Ca	Sc	Ti	V	Cr	Mn	Fe	Co	Ni	Cu	Zn	Ga	Ge	As	Se	Br	
5 = 5s 5d 5p 2×(1+3+5) = 18 elements		Kr	Rb	Sr	Y	Zr	Nb	Mo	Tc	Ru	Rh	Pd	Ag	Cd	In	Sn	Sb	Te	I	
6 = 6s 6f 6d 6p 2×(1+3+5+7) = 32 elements		Xe	Cs	Ba	*	Lu	Hf	Ta	W	Re	Os	Ir	Pt	Au	Hg	Tl	Pb	Bi	Po	At
7 = 7s 7f 7d 7p 2×(1+3+5+7) = 32 elements		Rn	Fr	Ra	**	Lr	Rf	Db	Sg	Bh	Hs	Mt	Ds	Rg	Cn	Nh	Fl	Mc	Lv	Ts

↓Period	Group →	18	19	20	21	22	23	24	25	26	27	28	29	30	31
6 = 6f 2×7 = 14 elements	*	La	Ce	Pr	Nd	Pm	Sm	Eu	Gd	Tb	Dy	Ho	Er	Tm	Yb
7 = 7f 2×7 = 14 elements	**	Ac	Th	Pa	U	Np	Pu	Am	Cm	Bk	Cf	Es	Fm	Md	No

Fig. 2. The Mudryk quantum table.

The chemical elements from atomic numbers 0 (ukrainium) through 117 (tennessine) have been discovered or synthesized, complete seven full rows of the periodic table. The periodic table consists of 118 cells arranged into 32 vertical columns and seven horizontal rows. The position of an element is given by quantum numbers. There are a total of four quantum numbers: the principal quantum number (n), the orbital angular momentum quantum number (l), the magnetic quantum number (m), and the electron spin quantum number (s).

In other words, the position of chemical elements in the table is determined by the configuration of electrons on the outer shell.

And in noble gases, all electrons are located on the inner shells. That is, the number of electrons in the outer shell is zero, they have zero valences. It follows that these chemical elements must present the zero period. D.I. Mendeleev did exactly that in his table, fig. 1. Because they are reluctant to share electrons from their filled inner electron shells, noble gases are generally considered unreactive.

In other words, in the newest Mudryk quantum table of the chemical elements developed by Ukrainian scientists Mudryk A., Kucherov O., Lavrovsky S. which is shown in figure 2 the position of chemical elements in the table is determined by the configuration of electrons on the outer shell.

Because of this, it is logical to place ukrainium in the zero group, as it has not the valence electrons.

In conclusion it should be noted that ukrainium Ua is a full chemical element, D. I. Mendeleev said that the zero element “cannot be in any way the world ether”. (Attempt of chemical understanding of the world ether. SPb., 1905)

UKRAINIUM IN NATURE

Ruling force in nature. Ruling forces exist in nature at the same time as working forces [3]. So any force F acting on the body B is divided into two components. As you know, the force acting on the body is decomposed into two components, this is the working force Fa , which acts along the movement and performs work, and the ruling force Fi , which acts across the movement and performs ruling, as figure 3 shows.

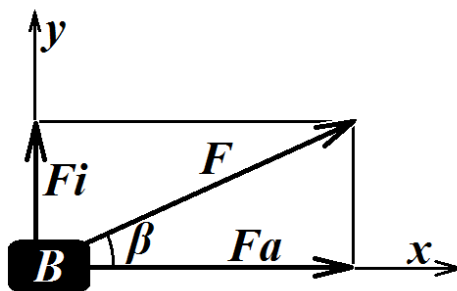


Fig. 3. The force F acting on the body B at an angle β to the direction of movement is divided into the working force Fa , which produces work, and the ruling force Fi , which performs managerial action.

Thus, the existence of two classes of forces should be taken into account in classical mechanics. The first class, $F_a = F \cos(\beta)$, is the working forces that act along the movement and perform work.

The second class, $F_i = F \sin(\beta)$, is the ruling forces that act across the movement, produce action, but do not perform any work. In other words, if the force vector \vec{F} is perpendicular to the motion $d\vec{r}$, then their scalar product will be equal to zero:

$$\vec{F} \cdot d\vec{r} = 0 \quad (2)$$

Here \vec{F} is the controlling force that does not perform work, $A=0$.

It is well known that the Lorentz force \vec{F} always acts across the direction of motion and, therefore, it does no work on a moving charge [7,10].

In this connection, we will consider the ruling force created by Lorentz force. This theory describes the fact of the presence of magnetic properties in revolving water molecules. The rotation of positive protons creates a solenoid, as shown on the figure 3. Direction of the magnetic field is determined by the rule of gimlet and magnetic induction B is created by Lorentz force:

$$B = \frac{mV}{qR}, \quad (3)$$

where m is the total mass of two protons, q is a charge of two protons, V is a linear speed of protons, and R — a radius of rotation.

Thus, the equation notes the fact of the presence of magnetic properties in revolving water molecules.

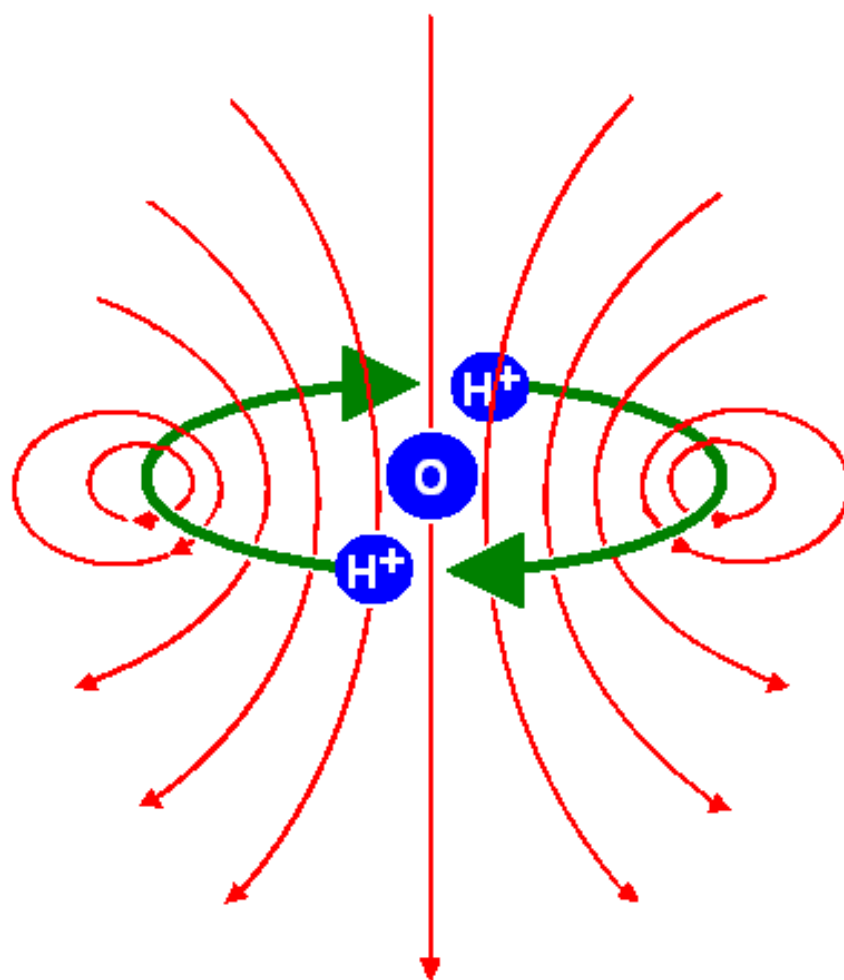


Fig. 4. Solenoid. The rotational motion of positively charged protons around the negatively charged atom of oxygen creates the magnetic field.

Figure 4 shows the solenoid. The rotation of positive protons in the water molecule creates it. The solenoid is created by one rotary magnetic molecule. Many rotating magnetic molecules interact with each other and create collective magnetic field with great number additional properties. This state is possible owing to the fact that integral equalization of Ampere the methods of the field theory [2].

The ruling force, or Lorentz force, is able to organize motion of magnetic dipoles. The ruling force is got from the Ampere equalization by the field theory methods.

Problems of the thermodynamics model. Among all natural catastrophes which take place on Earth, the greatest danger is caused by hurricanes/cyclones. Long-term studies conducted by the National Hurricane Center, Colorado State University, National Oceanic, Atmospheric Administration and many other groups [5], allow us to learn deeply the spectral and thermodynamic materials. But as there is no adequate model, the frontal attack on the hurricanes, adopted by “Storm Fury” and conducted for twenty years – from 1963 to 1983 – ended in a failure.

Extensive research allowed us to investigate the causes and births of hurricanes zones, height and ways of movements, to describe their structure and dynamic. These “pricks” for a whirlwind energy which is about 10^{17} J with a frontal closeness about 100 J/cm^2 were rather weak. Atlantic basin seasonal hurricane investigations allowed us to build a capable working model of prognoses of hurricanes appearances.

As a result of wide research of birth, development, and fading of hurricanes, the volume of various measuring of physical parameters is accumulated. Repetition of data confirms their high truth. These results show that in hurricanes there are such processes which thermodynamics theory is not able to describe. We will specify them. Warm, dry, and transparent air in the eye of hurricane comes down from troposphere, becoming moist and cold near the surface of the ocean [23]. Moist and cold air rises from the surface of the ocean along the eye wall of a hurricane with an increasing speed creating here a tangential force to wind [17, 18].

Hurricanes make highly charged electric clouds which can burst by lightings. Hurricanes rotate in opposite directions in different hemispheres, and the Earth magnetic field is opposite in two hemispheres. During the most studies, Gulf of Mexico hurricanes tend to migrate dominantly northward in the Earth magnetic direction field [24]. If the hurricane forms a giant system of magnets, this behavior seems to be logical.

The ukrainium creates a hurricane eye wall. For this reason, examining Lorentz force as that organizes motion in some set direction, many difficult phenomena of nature become clear. It is shown that the ruling force gives power to the hurricanes/cyclones, comets and astrophysical masers. This statement is confirmed in a number of facts. The results of visible, infrared, and radio spectrometry are written done by ruling force theory. It describes adequately, in details polarization and the masses spectral dates.

The implementation of ruling force in science gives substantial results. For example, it improves functional possibilities and increases an efficiency of the system that prepares engine’s air – fuel mixture.

An electric motor uses energy of magnetic field to produce a mechanical work; it is very typical through the interaction with ions of H^+ and OH^- . Ions are pushed from the magnetic field to the maser cloud, it is executed in accordance with the plasma theory.

Figure 4 shows both the chart of laboratory laser pumping, the picture on the left and astrophysical maser pumping, the picture on the right.

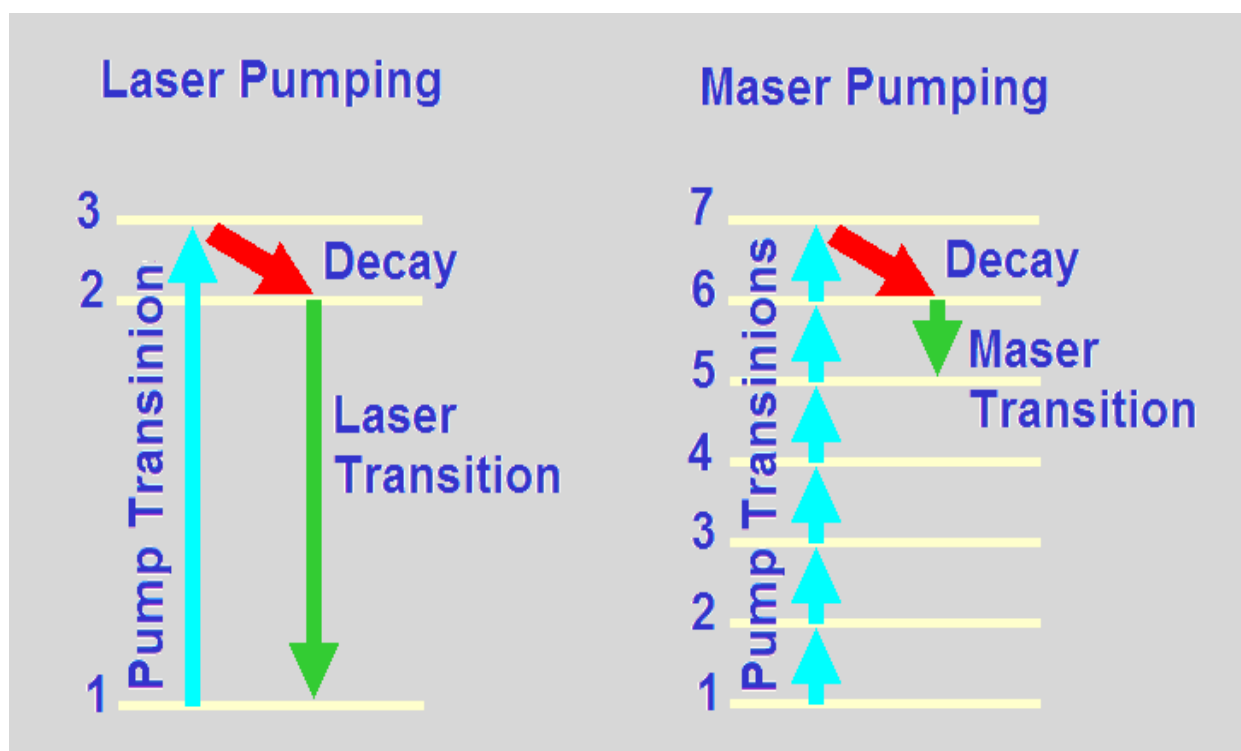


Fig. 5. The pumping schemes of the laboratory laser and the astrophysical maser [2].

The inversion of populated of levels in the laboratory laser pumping is got by means of visible light of pumping. The light is absorbed by the active medium so that the molecules are pumped from lower laser level to the upper laser level; it is level 2 on Figure 3. The laser transition takes place from the upper level 2 on the lower level 1.

Figure 5 shows a hurricane model obtained from the theory of information physics, which will be presented below, by the method of solving Ampere's integral equation.

According to this theory, the rotational movement of water molecules that have crossed the inversion layer in a hurricane acquires a high speed.

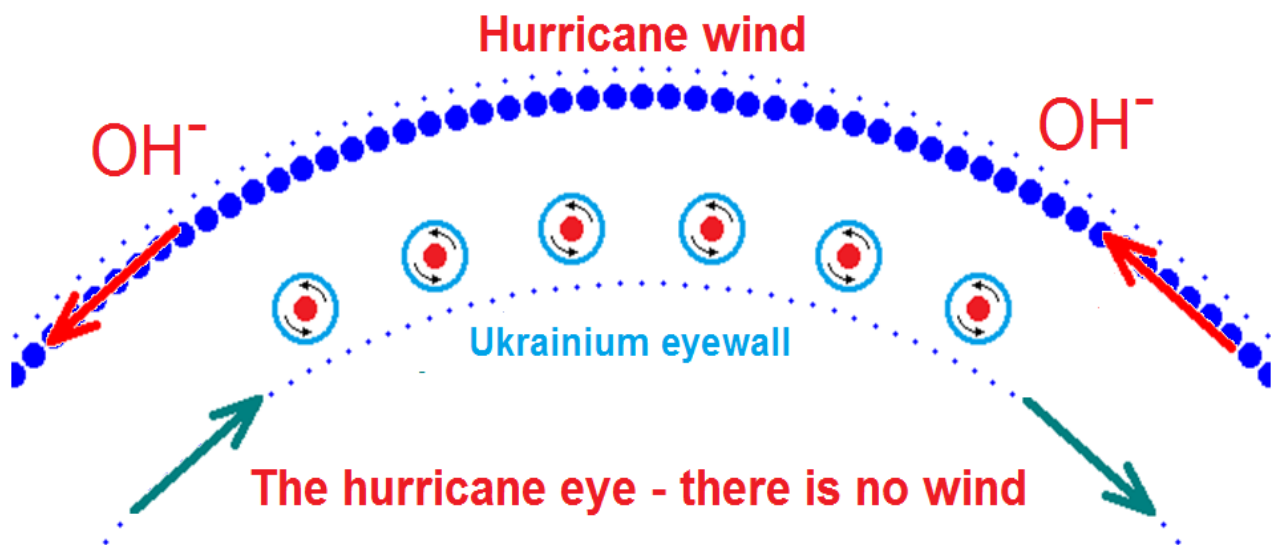


Fig. 6. Diagram of operation of the Hurricane Nano engines.

The centrifugal forces begin to exceed the valence bonding, the energy of which is 23 kJ/mol, and the H₂O molecule breaks into an H⁺ proton and an OH⁻ group. As a result, the H⁺ protons move with a velocity of 28 km/s in a clockwise direction, and the OH⁻ group moves with a velocity of 5.3 km/s in the opposite direction. The energy of the rotational motion of the water molecule is transferred to the tangential wind of the hurricane.

Figure 6. View of a hurricane from space, with a cylindrical wall in the center, which consists of ukrainium. The OH⁻ group, this is the cargo of the Nano Engine. It creates a hurricane wind with an initial velocity of 5.3 km/sec.

Figure 6 shows a view of the hurricane from space. Figure 5 shows a view of the hurricane from space. In the center, the wall of the hurricane eye can be seen. As shown in the diagram above, the ukrainian Ua forms the eye wall of the hurricane and acts as a support for the hurricane wind. If the hurricane's engine is the water molecules (wheels), the train is the cargo (hurricane tangential wind), the support is the railway [11].

Thus, the hurricane eye wall consists of a hitherto unknown substance with the following properties: 1) it is a solid material with properties of metal; 2) it has the shape of a hollow cylinder; 3) the wall thickness is less than a nanometer; 4) the cylinder rotates at a speed of 28 km/s; 5) it is sealed; 6) its lifetime is not limited.

The studies of hurricanes by a spectral technique (polarimetry, infrared and mass spectroscopy) have showed that the ruling material force make the warm water molecules become an energy source of hurricanes [8, 9].

The theory describes the fact of the presence of magnetic properties in revolving water molecules. The rotation of positive protons creates a solenoid, as shown on figure 7. The informing reality process forms a giant system of magnets. Solenoids cluster along the lines of the magnetic field, thereby creating an anisotropic environment that changes the polarization of light, as shown on

figure 7. It is possible to assert that the magnetic acceleration of the rotational motion of a water molecule creates powerful infrared radiation. It is known that this global atmospheric phenomenon is accompanied by an anomalous increase of intensity at the frequency of 22.24 GHz. It is the frequency of the rotational spectrum of the water molecule. Meteorological satellites work in this spectral range, as shown on figure 7.

According to the theory suggested by the author, the rotational motion of water molecules which have crossed the inversion layer in the eye of hurricane acquires a high speed.

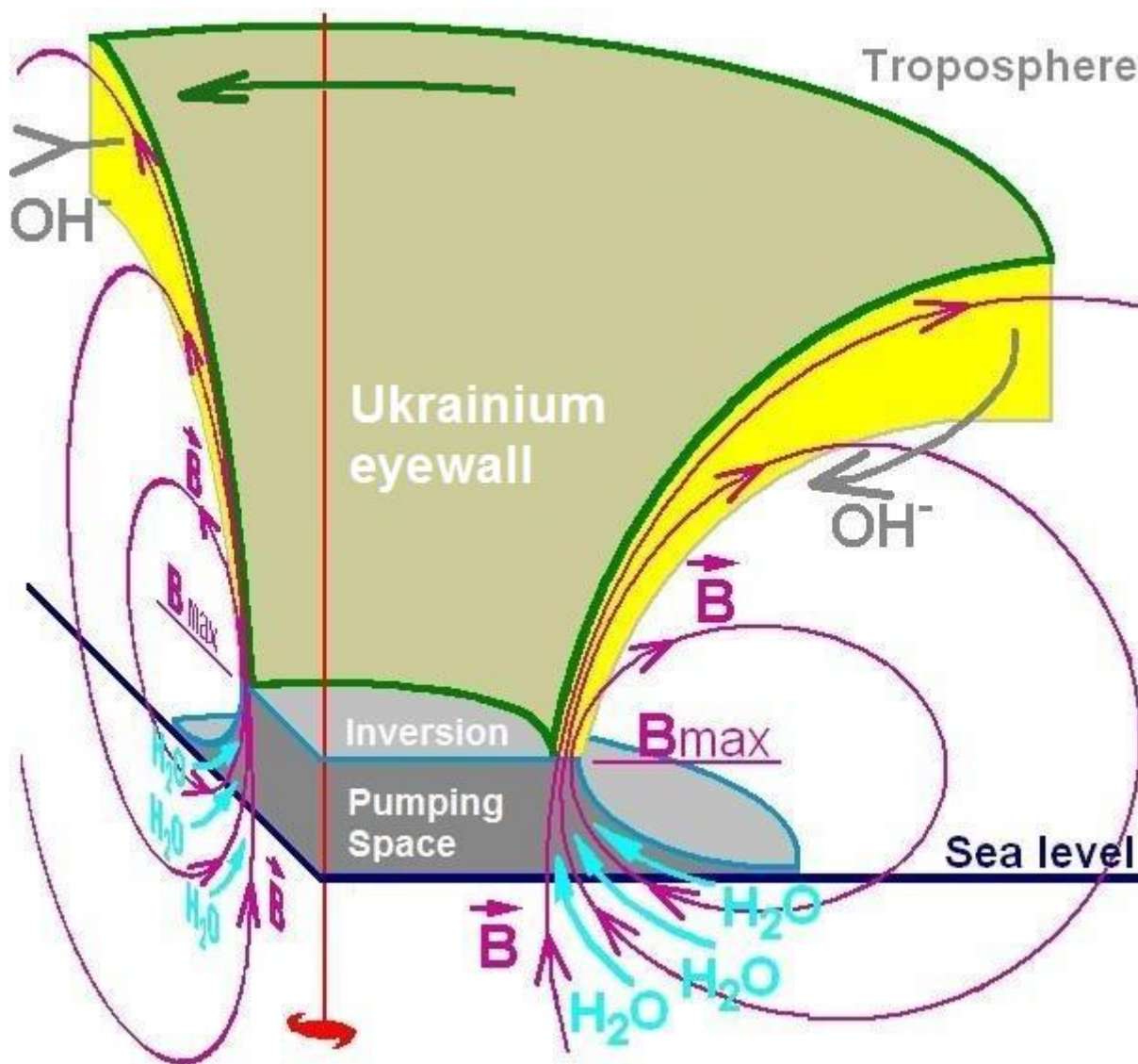


Fig. 7. The hurricane/cyclone power system [12].

The hurricane eye wall consists of the ukrainium.

Centrifugal forces begin to exceed the valence bond and the H₂O molecule is torn into the H⁺ proton and the OH⁻ group. As a result, the energy of the rotational motion of the water molecule is

passed to the tangential wind of hurricane. Protons are moved by the eyewall of hurricane to the troposphere and form a proton cloud there.

According to L.D. Landau [16], the entropy cycle still exists and it must be sought in the field of general relativity, since the Universe is a system that is in a variable gravitational field, the law of increasing entropy is not applicable to it.

The hurricane green energy [6] is renewable and environmentally friendly [13] and it can be used in the Ukraine [14].

The ukrainium is found in the Earth's atmosphere. This result is based on the mass spectroscopy detection technique, which was implemented on the shuttle Discovery in 1998, as shown on the figure 8.

The suggested theory exposes the nature of the self-formation of a hurricane, specifies its forces, and adequately describes its parameters.

Mass spectroscopy. As shown in figure 4, protons move by the eye wall of hurricane to the troposphere and form proton clouds there.

This result is based on the mass spectroscopy detection technique, which was implemented on the shuttle Discovery in 1998 [15].

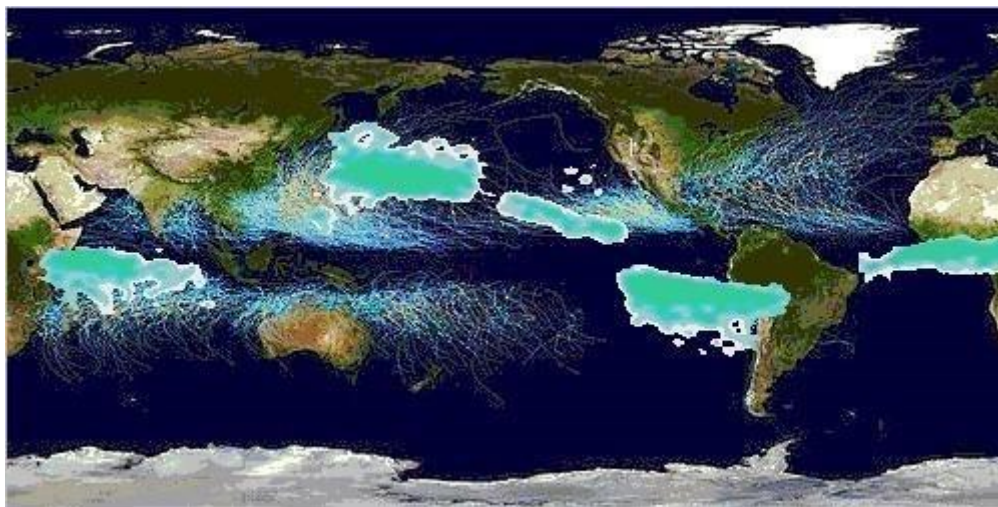


Fig. 8. Accumulation of the uranium in the Earth's atmosphere [15].

The location of protons clouds correlates strongly with the ways of hurricanes, which are given by points [10, 12].

The expounded theory describes spectral data as well as thermodynamic materials [9].

VISUALISATION OF THE URANIUM ATOMS BY MEANS OF PICOSCOPY

Unlimited possibilities of the picoscopy. The picoscopy makes it possible to visualize the atoms and molecules of various substances in real life.

Picoscopy is a visualization technology of the atomic universe. With our PICOSCOPY technology we can look beyond what is achievable with modern science and electron microscopes and create new materials at the PIKO level!

On the basis of the PICOSCOPY technology it is possible to produce chips at 0.01 nm!

To make new types of materials such as transparent bulletproof metals with a thickness of 0.1 mm!
And much more!

New knowledge in the field of pico-scopy will make it possible to create new drugs and new fuels, including super-efficient rocket fuel for launching rockets into space and to distant Mars. As well as fuel for heating private households by liquid fuel boilers, this is extremely environmentally friendly. New types of environmentally friendly gasoline based on methanol and hyper isooctane and n-heptane and multi-dimensional more hydrogen-rich hydrocarbon fuels will greatly reduce air emissions.

Researchers divide petrol into two main chemical components - isooctane (an aliphatic hydrocarbon) and n-heptane (an alkane) - whose proportions are crucial for determining the octane number. If we know the quantity and formula of these two substances, we can calculate the mass ratio of the substance to the amount of fuel. Also with the help of picoscopy science it is possible to develop technologies for hydrogenation of isooctane and n-heptane (alkane) nases and attachment of more hydrogen to carbon molecules, thus improving energetic and ecological parameters of vehicle fuels. To improve marine fuel oil, this is terribly polluting to the atmosphere of planet Earth. Picoscopy technology can significantly improve the environmental performance of bunker fuels, reducing CO₂ and carbon emissions by 40-80 per cent.

For human health, explore and understand more deeply the molecular interactions of drugs based on the new science of picoscopy and improve their properties to improve the therapeutic properties of drugs and reduce the detrimental chemical effects on the body. Develop novel nano- and pico-targeted medicines.

PicoScopy provides visualization of molecules and gives scientists the latest technological tool to work on developing and accurately pinpointing new material properties.

PicoScopy will provide a major boost to breakthroughs in creating new superconducting and ultrafast computers, including quantum computers. It will provide a creation of new superstrong materials such as new metal glass 5-8 times stronger than armor.

The newest science of picoscopy will bring to science and technology a new scientific and economic point, comparable to the Curie's discovery of radioactivity and the creation of new tools for understanding chemistry and physics and creating new materials and equipment, a breakthrough in the development of pico-electronics and quantum computers. For the economy, this translates into a multibillion-dollar gain. For scientists, new breakthroughs in the development of humanity!

The ukrainium in the pentane molecule. By definition, in an ionic bond, one of the chemical elements completely gives up an electron to another element. Based on this definition, in the model of C₅H₁₂ pentane, presented in Figure 9c, there are no electron clouds around 12 proton nuclei. They have completely moved to the carbon atom. It follows that figure 9b shows the wrong pentane

model. Conclusion: all models of water, alkalis, acids, organic substances that have an ionic bond with hydrogen so they must be redrawn and brought into line with reality.

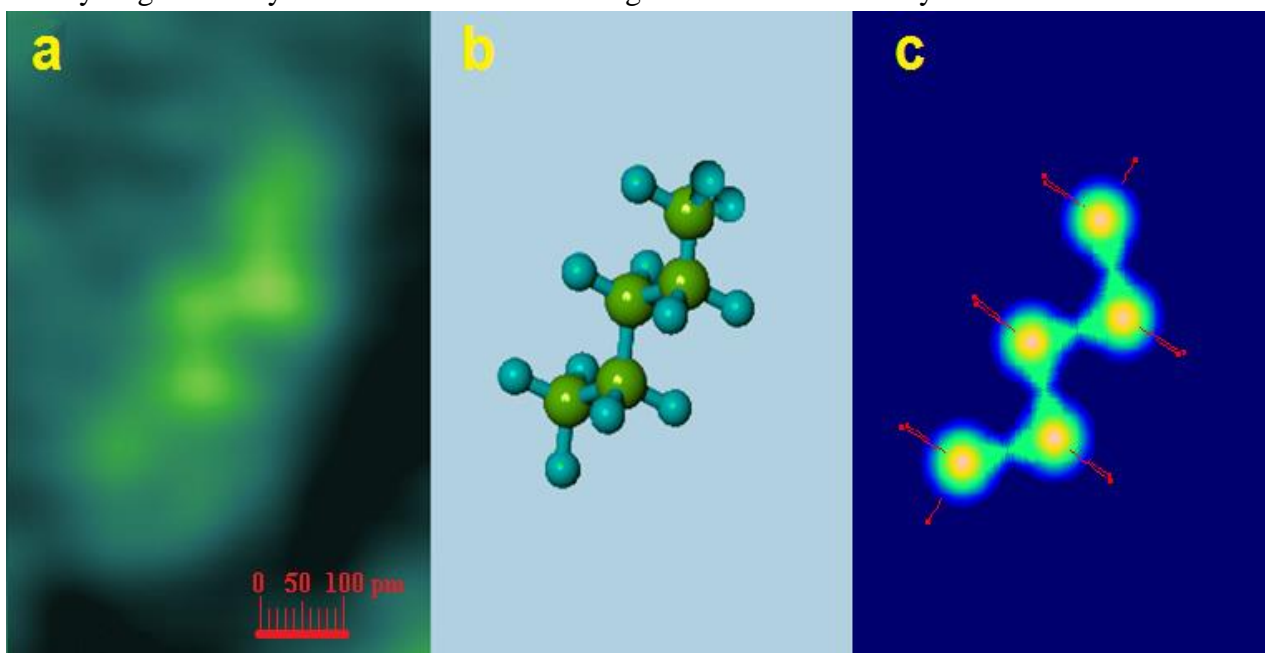


Fig. 9. One single molecule of pentane C_5H_{12} : a) atomography with a resolution of 10 pm [4]; b) wrong model of the pentane; c) true model of the pentane when the atoms of uranium (red points) have not the electron body.

Figures 9 show a C_5H_{12} pentane molecule. Figure 9a shows the atomography of the electron clouds densities $\rho(x, y)$ of the molecule with resolution of 10 pm. The atomography shows all five electron clouds around the carbon atoms of the pentane molecule. According to the laws of quantum mechanics, the nucleus of hydrogen atoms devoid of electron clouds and, accordingly, hydrogen atoms are invisible in the atomography. The bond length between carbon atoms in the pentane molecule is 154 pm and the angle between them is 112° . Figure 24b shows a model of the C_5H_{12} pentane molecule, obtained as a result of X-ray diffraction analysis.

Every carbon atom in the pentane molecule has ten electrons, just like a neon noble gas.

The three inside carbon atoms have two strong sp hybrids of the covalent bonds (green) and two ion bonds from hydrogen atoms (red):

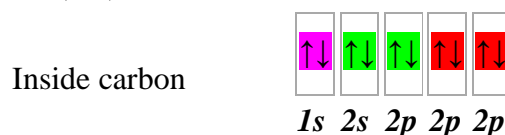


Fig. 10. Sp hybrids in inside carbon.

The two outside carbon atoms have one s hybrid of the covalent bond (green) and three ion bonds from hydrogen atoms (red):

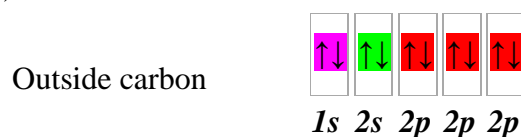


Fig. 11. S hybrid in outside carbon.

These results demand a rethinking of all organic chemistry.

Conclusions

The ukrainium starts the D.I. Mendeleev's table and finishes it formation.

The material expounded in the manuscript confirms once again, that the laws of materialistic dialectics with identical force operate both in the economic and in the physical spheres.

The theory and interpretation presented here suggest strongly that the powers both in economy and in nature are divided into two classes: working class and ruling class. The ruling power obeys the following law: knowledge is power which rules the motion without implementation of any work.

Ruling power in economy, called "Professional and Managerial Class", is defined by the organizing function it plays in the reproduction.

Ruling power in nature, which always operates across direction of motion, exists and is generally known. It is Lorentz force. The ruling force (or Lorentz force) exists independently, out of human consciousness.

Thus, on condition that we examine Lorentz force, as power that organizes motion in some directions; many difficult phenomena of nature become clear. The ukrainium gives force to the hurricanes/cyclones, comets, and astrophysical masers. The theory allows describing qualitatively and quantitatively the enormous amount of measurement of all these various phenomena of nature.

As it has been shown in the manuscript, the ukrainium has wide distribution in nature. It can often be found in the atmosphere of Earth, in the sunny system, in galaxies, and in intergalactic space.

All things considered, on the question of Engels to Darwin: does nature choose?

The power of knowledge allows us to give the negative answer:

No, nature does not choose, - on the contrary, nature rules.

References

1.O.P. Kucherov. THE ZERO ELEMENT OF THE D.I. MENDELEEV'S PERIODIC TABLE CAN STOP ANY HURRICANE. Information technology and special security (2020), 16–59 (<https://science-ua.com/gallery/maketn6.pdf>)

2.Kucherov, Olexandr. Power of knowledge in economy and nature: knowledge is power, which creates the organized motion and never implements any work / Saarbrucken : LAP LAMBERT Academic Publ., 2014. - 57 p.

3. Engels F. Dialectics_of_Nature // http://www.marxists.org/archive/marx/works/download/ngelsDialectics_of_Nature_part.pdf

4. Erik Olin Wright, Varieties of Marxist Conceptions of Class Structure//Politics &

5. Klotzbach Philip J., "On the Madden-Julian Oscillation-Atlantic Hurricane Relationship," *Journal of Climate* 23, 282–293 (2010).
6. Kuchеров О. The Nature of Hurricane Green Energy // *Proceedings of the 8-th International Green Energy Conference, Monograph, NAU, Kyiv-2013.* — P.317-320.
7. Kuchеров О. Power of knoweledge, which maneges direction of motion in economy and nature // *Jornal of Qafqaz University. Mathematics and Computer Science.* №1, 2013, p. 24-30.
8. Kuchеров O.P., Pazdriy Y.E., Fuel Feed Device of an internal combustion engine. Patent of Ukraine № 90406 (2008).
9. Kuchеров O. P. and Pazdriy Y. E. Advanced hurricane studies by a spectral detection technique: polarimetry, infrared and mass spectroscopy// NATO ASI "Spectral Detection Techcique (Polarimetry) and Remote Sensing" Kyiv, Ukraine, 12-25 September 2010.
10. Kuchеров O.P., Pazdriy Y.E., Information Substance Decreasing Entropy of a Complex System // *Actual Problems of Economics, Scientific Economics Journal.* — 2010. — №9. — P.300-304.
11. Kuchеров O.P., Pazdriy Y.E., Informative Reality, as a Mean of Hurricanes Managment // *Actual Problems of Economics, Scientific Economics Journal.* — 2011. — №2. — P.214-221.
12. Kuchеров O.P., Pazdriy Y.E., Edvanced Hurricane Studies by Spectral Detection Technique: Polarimetry, Infrared and Mass Spectroscopy // *Astronomical School's Report.* 2011.— №1-2. — P.48-55.
13. Kuchеров O.P., Pazdriy Y.E., Use of Information reality in the Ecological Management System // *Actual Problems of Economics, Scientific Economics Journal.* — 2012. — №1/2. — P.129-136.
14. Kuchеров O.P., Pazdriy Y.E., Economic evaluation of the Informative Reality Influencing on Energy Consumption in the Ukraine // *Actual Problems of Economics, Scientific Economics Journal.* –2011. – №7. –С. 307–313.
15. Luchkov B., "Hurricanes are eternal problem," *Science and life* 3, (2006).
16. Ландау, Л. Д., Лифшиц, Е. М. Статистическая физика. Часть 1. — Издание 3-е, дополненное. — М.: Наука, 1976. — 584 с. — («Теоретическая физика», том V), §8.
17. Shapiro, L. J., Willoughby H. E., "The response of balanced hurricanes to local sources of heat and momentum," *J. Atmos.Sci.* 39, 378–394 (1982)
18. Schubert, W. H., and Hack J. J., "Inertial stability and tropical cyclone development," *J. Atmos. Sci.* 39, 1687–1697 (1982).
19. Shea Dennis J., Gray Willam M. "The Hurricane's Inner Core Region," *Journal of the Atmospheric Sciences* 30, 1544–1564 (1973).
20. Thomson, W. (1851) "On the dynamical theory of heat; with numerical results deduced from Mr. Joule's equivalent of a thermal unit and M. Regnault's observations on steam" *Math. and Phys. Papers* vol. 1, pp 175–183
21. Tropical Cyclone. // <http://ru.wikipedia.org/wiki/>
22. Weaver H., Dieter N.H., Williams D.R.W., Lum W.T. 1965 *Nature* 208 29-31
23. Willoughby H. E., "Tropical Cyclone Eye Thermodynamics," *Mon. Weather Rev.* 126, 3053–3067 (1988).
24. Willoughby, H. E., "Temporal changes in the primary circulation in tropical cyclones," *J. Atmos. Sci.* 47, 242–264 (1990).

Kucherov O.P., Lavrovsky S.E.

VISIBLE ATOM

Institute of Structural Information Technologies, Kyiv, Ukraine

E-mail: O.Kucherov@i.ua

Reference: O.P. Kucherov, S.E. Lavrovsky, Visible atom. Information technology and special security (2022), 29–62 (<http://science-ua.com/gallery/maketn8.pdf#page=29>)

The review is devoted to the breakthrough in fundamental physics made by the authors, namely the discovery of the unexpected natural phenomenon when the electron beam passing through the electron cloud shifts toward its center under the influence of quantum superposition. The shift effect causes atoms, molecules and chemical bonds to glow in proportion to the electron clouds density creating an atomography.

The review presents atomographs of the atoms in various substances. In frequency, atomography of a carbon atom clearly shows clouds of each of the six electrons. Atomographs are shown for all carbon allotropes. The atomography allowed us to discover a number of new allotropes of carbon, such as superdense substance rudenite, superthin diamond gubanete and non hybridized Musokhranov coke.

With the advent of the atomography, the blind sciences for which the subject of study was a mystery for a long time, become sighted: visible chemistry; visible molecular physics; visible resistance of materials; visible physics of semiconductors; visible microelectronics; visualization of quantum dots. Direct visualization of atoms opens limitless horizons of possibilities for these new sciences.

Keywords: *electron beam shifting effect; electron cloud densitometry; molecule; atom; chemical bond; picoscopy; atomography; visible chemistry; visible molecular physics; visible resistance of materials; visible physics of semiconductors; visible microelectronics; visualization of quantum dots; rudenite; gubanete; Musokhranov coke.*

Кучеров О.П., Лавровский С.Е.

ВИДИМІЙ АТОМ

Огляд присвячений прориву авторів у фундаментальній фізиці, а саме відкриттю несподіваного природного явища, коли пучок електронів, проходячи через електронну хмарку, зміщується до її центру під дією квантової суперпозиції. Ефект зміщення електронного променя змушує атоми світитися пропорційно до щільності електронних хмар і створює атомографії: молекул, атомів і хімічних зв'язків.

В огляді представлені атомографії атомів у різних речовинах. Показано атомографію атома вуглецю з усіма шістьма електронами. Наведено атомографії для всіх алотропів вуглецю. Пікоскоп дозволив виявити низку нових алотропів вуглецю, таких як надщільна речовина руденет, надтонкий алмаз губант і негібридизований кокс Мусохранова.

З появою атомографії сліпі науки, для яких предмет вивчення довгий час був загадкою, стають зрячими: видима хімія; видима молекулярна фізика; видимий опір матеріалів; видима фізика напівпровідників; видима мікроелектроніка; візуалізація квантових точок. Пряма візуалізація атомів відкриває безмежні горизонти можливостей для цих нових наук.

Ключові слова: *ефект зсуву електронного променя; денситометрія електронної хмари; молекула; атом; хімічний зв'язок; пікоскопія; атомографія; візуальна хімія; візуальна молекулярна фізика; візуальний опір матеріалів; візуальна фізика напівпровідників; візуальна мікроелектроніка; візуалізація квантових точок; руденіт; губант; кокс Мусохранова.*

Кучеров А.П., Лавровський С.Е.

ВИДИМЫЙ АТОМ

Обзор посвящен прорыву авторов в фундаментальной физике, а именно открытию неожиданного природного явления, когда пучок электронов, проходя через электронное облако, смещается в его центр под действием квантовой суперпозиции. Эффект смещения заставляет атомы светиться пропорционально плотности электронных облаков и создает реальные атомографии: молекул, атомов и химических связей.

В обзоре представлены атомографии атомов в разных веществах. Показана атомография атома углерода со всеми шестью электронами. Приведены атомографи для всех аллотропов углерода. Пикоскоп позволил обнаружить ряд новых аллотропов углерода, таких как сверхплотное вещество руденет, сверхтонкий губант алмаз и негибридизованный кокс Мусохранова.

С появлением атомографии слепые науки, для которых предмет изучения долгое время был загадкой, становятся зрячими: видимая химия; видимая молекулярная физика; видимое сопротивление материалов; видимая физика полупроводников; видимая микроэлектроника; визуализация квантовых точек. Прямая визуализация атомов открывает безграничные горизонты возможностей для этих новых наук.

Ключевые слова: *эффект смещения электронного луча; денситометрия электронного облака; молекула; атом; химическая связь; атомография; пикоскоп; визуальная химия; визуальная молекулярная физика; визуальное сопротивление материалов; визуальная физика полупроводников; визуальная микроэлектроника; визуализация квантовых точек; руденит; губанит; кокс Мусохранова.*

Table of contents

Introduction

1. INVISIBLE ATOM

1.1. History of the doctrine of atoms

1.2. Are atoms really invisible?

2. VISIBLE ATOM

2.1. Molecules tell about their form

2.2. Quantum theory of the electron beam shifted effect

2.3. Fundamental difference from the transmission

3. VISIBLE CARBON ATOM

3.1. Graphite

3.2. Graphene

3.3. Diamond

3.4. Nanotubes

3.5. Rudenete

3.6. Gubanete

3.7. Active coal

4. VISIBLE ATOM TECHNOLOGY

4.1. Visible chemistry.

4.2. Visible molecular physics

4.3. Visible resistance of materials

4.4. Visible physics of semiconductors

4.5. Visible microelectronics

4.6. Quantum dots visualization

Conclusion

References

Introduction

Universe consists of atoms. All compounds that surround us, with which we deal and make up our body - consist of atoms.

Atoms surround us everywhere, both in nature and in everyday life. Atoms with help chemical bonds create thousands of different molecules, and we are well aware of their properties, composition and geometry. Atoms form the basis of science and technology.

For three thousand years, scientists all over the world have had one unrealizable dream - to see the atoms, those particles that make up everything.

This possibility is provided by a fundamental discovery in the field of visualization of the smallest particles in the world, which retain the ability of matter. As a result of the work on comparing the properties of matter and space, the authors managed to discover a unique phenomenon when an atom shift electron beam towards the highest density. This property leads to a fantastic result - the atoms begin to glow, visualizing their form in all its diversity.

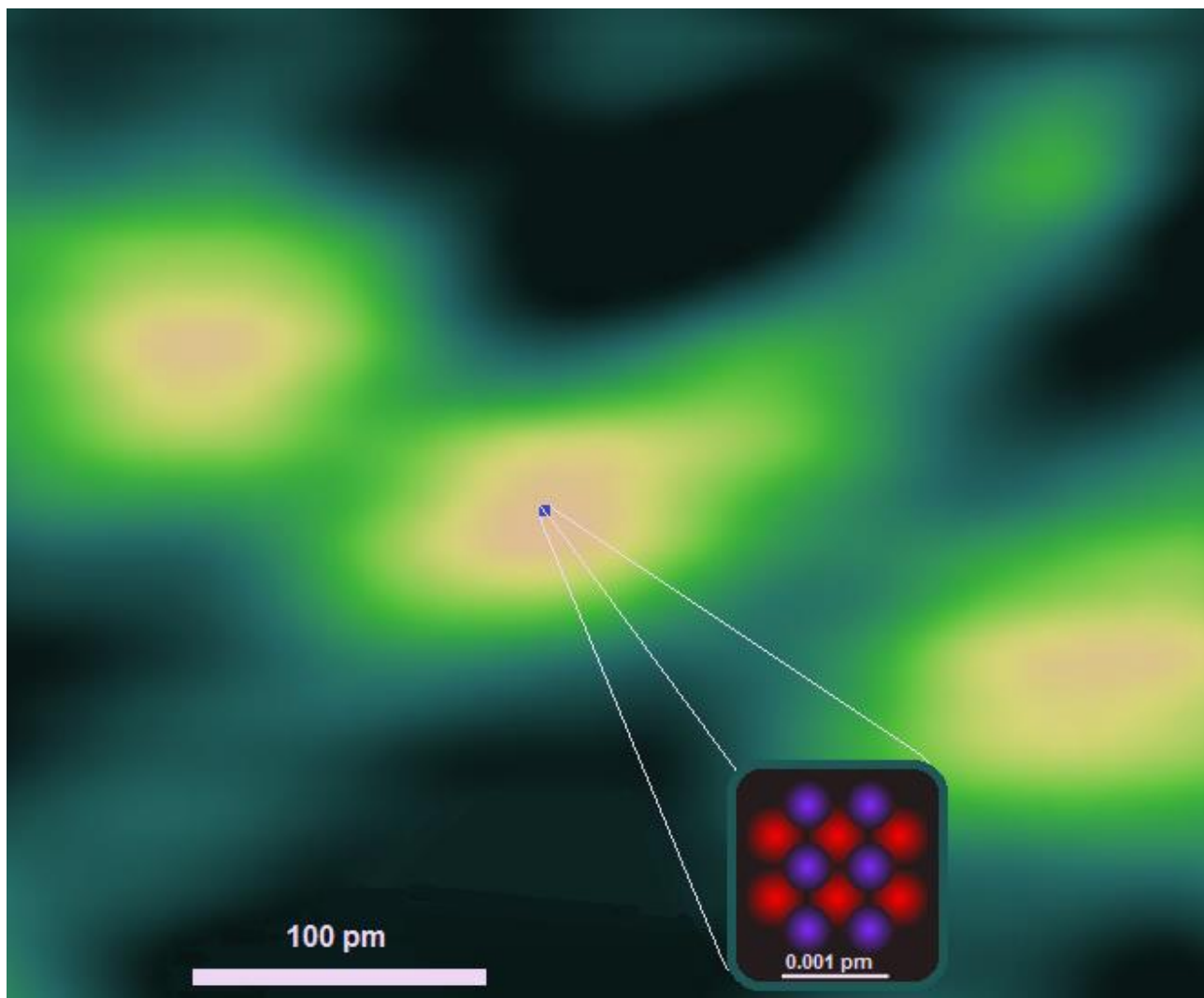


Fig. 1. Atomography of a carbon atom with six electrons: two pink inner electrons; two green covalent electrons and two blue active electrons.

The eternal dream of mankind has come true - to see the internal structure of the nature around us. This breakthrough of humanity into picocosmos was unexpected; it was not mentioned either in scientific works or in science fiction writers.

1. INVISIBLE ATOM

Atoms have not been seen for 3,000-year.

1.1. History of the doctrine of atoms

The term "atom" was introduced into scientific circulation by **Democritus** about 3,000-year-old. Democritus believed that atoms were uniform, solid, hard, incompressible, and indestructible and that they moved in infinite numbers through empty space. All atoms have a certain shape and atoms of same substance are identical.



Democritus

One of the first theories about the structure of atoms, which already has modern outlines, was described by G. Galileo (1564-1642). According to his theory, matter consists of atoms that are not at rest, but move in all directions under the influence of heat; heat is nothing but the movement of atoms. The structure of the atoms is complex. G. Galileo was the first to present the structure of atoms in a hypothetical form.

D.I. Mendeleev in 1869 discovered the Periodic Law - a fundamental law of nature that determines the properties of atoms, as well as the composition and properties of substances that are in a periodic dependence on the values of the charges of the nuclei of the atom.

In 1897 J. J. Thomson, studying cathode rays, discovered the electrons and came to the conclusion that they are a component of every atom, the Nobel Prize in Physics 1906. The existence of the electron showed that the 3,000-year-old conception of the atom as a complex particle was right and the atom consists of many different and connected parts.

The planetary model of the atom was created by Ernest Rutherford (Nobel Prize in 1908). He proved that the positive charge and the bulk of the atom are in a small nucleus. The negatively charged electrons revolving around the nucleus create the material shell of every atom.

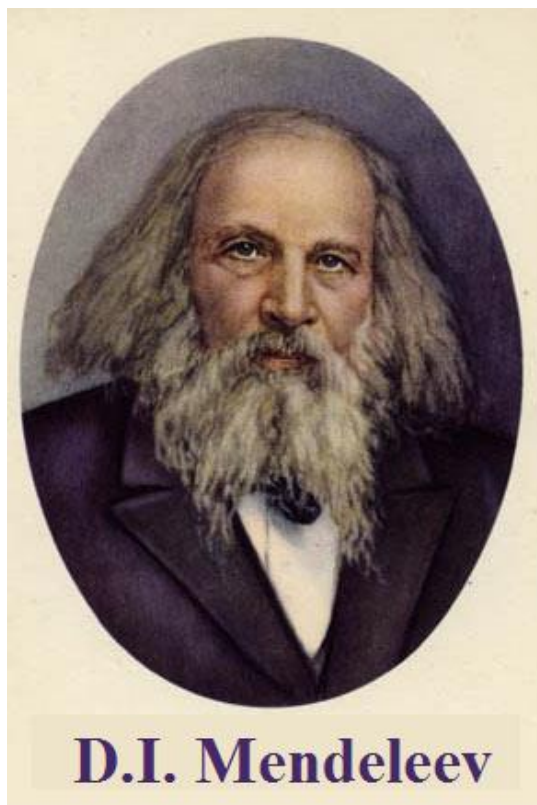
Niels Bohr in 1913 built the quantum theory of the atom (Nobel Prize 1922). Bohr's theory led to the creation of quantum mechanics, which explains the optical spectra of atoms.

Erwin Schrödinger, Paul Adrien Maurice Dirac and others led to the full development of quantum mechanics in the mid-1920s, which showed the rotational motion of light electrons around a heavy nucleus and the absence of orbital electrons. Electrons fill the entire volume of the atom. The Nobel Prize in Physics 1933 was awarded jointly to Erwin Schrödinger and Paul Adrien Maurice Dirac "for the discovery of new productive forms of atomic theory."

In this regard, Richard Feynman proposed to consider an atom in the form of a cloud, whose density is proportional to the probability density for observing the electron. Thus "picture" of an atom is a nucleus surrounded by an "electron cloud" [6], the Nobel Prize in Physics 1965.

An available method for studying the molecular structure of a substance is X-ray diffraction analysis. The theoretical substantiation of the method was given by G. V. Vulf and V. L. Bragg (Nobel Prize in 1915). The method is based on the phenomenon of X-ray diffraction on a three-dimensional crystal lattice.

For determining the structure of substances by X-ray diffraction analysis, the Nobel Prize was awarded to P.I.V. S. Mulliken 1966, G. Herzberg 1971, A. Klug in 1982, G. A. Hauptman 1985.



For the development of ultra-high resolution fluorescence microscopy, the Nobel Prize (2014) received by E. Betzig, W. Merner, S. Gell.

The world pinnacle in the study of molecular structures was the award of the Nobel Prize (2017) in chemistry to Jacques Dubochet, Joachim Franco and Richard Henderson for the development of low-temperature electron microscopy of biomolecules organized into structures by electron beam scattering.

A wide range of research made it possible to obtain a lot of information about the structure and properties of atoms, however, the atom still remained invisible.

1.2. Are atoms really invisible?

Why have we not yet seen the *material shell* (Rutherford) or *electron cloud* (Feynman) of every atom? Let's consider the root of the problem. The basis question is: what is the ability to see any object around us?

The ability to see surrounding objects is endowed with humans, animals, fish and insects due to the presence of eyes. Optical devices improve our vision. These are cameras, telescopes, microscopes. All of them use electromagnetic waves - light, radio waves, gamma radiation and elementary particles (electrons, protons). Eyes and optical devices work according to the laws of wave optics. For this, the body must change the wave. These are reflection (for example flowers); absorption (for example a safety glasses) or scattering (for example clouds in the sky). Thanks to wave optics, we have the opportunity to see both the macrocosm of stars and galaxies and the microcosm of objects around us, up to bacteria.

The fact is that an electron cloud of an atom completely passes the wave. That is, it is impossible to see an atom by means of wave optics. Optical devices cannot, in principle, visualize the shape of an atom.

Finally, the picoscopy made the atom visible, realizing the 3,000-year-old dream of all mankind.

2. VISIBLE ATOM

Atoms have become visible starting from February 27, 2018 thanks to the discovery of picoscopy [9].

Ukrainian physicist O.P. Kucherov and engineer I.E. Lavrovsky made the visualization of molecules thanks to a fundamental discovery in the fields of quantum mechanics and unique technique.

First, it was experimentally discovered the unexpected natural phenomenon of electron beam shifted by a three-dimensional electron cloud. [7].

Secondly, using the methods of theoretical physics, the authors proved that the phenomenon of electron beam shifted by a three-dimensional electron cloud is an action of quantum superposition [10].

Thirdly, the result was picoscopy which gives atomographs of pico-size objects: molecule, atoms and chemical bonds [9].

Let's describe all three steps in detail.

2.1. Molecules tell about their form

The ability of atoms to shift an electron beam was experimentally discovered by Ukrainian physicist O.P. Kuchero and engineer I.E. Lavrovsky [7], this phenomenon is purely quantum mechanical and unknown in optics. Indeed, an individual atom is unable to absorb, reflect, or scatter a beam. However, as it turned out by the authors, in accordance with the principle of superposition the electron beam shifts in the direction of increasing the electron density in atoms. As a result, the electron shell begins to glow against the dark background of the space in which the molecule is located, conveying the shape of molecules in all details. The shift of the electron beam is in full accordance with the principle of superposition, which is the basis of quantum mechanics.

The fundamental basis of quantum mechanics is the Heisenberg uncertainty principle, which captures a simple fact of life: an electron beam that has passed through a measuring device carries information about it. The authors found that the electron beam receives information about the shape of the electron cloud of the atom through which it passes.

2.2. Quantum theory of the electron beam shifted effect

The following describes the theory of electron cloud densitometry of atoms and chemical bonds.

The body of electrons cannot be seen with either an optical microscope or a transmission electron microscope. Classical physics does not allow this.

However, quantum mechanics allows us to observe the real shape of the inner and valence electrons. Quantum mechanics teaches that the electrons that revolve around the nucleus of an atom have the shape of a cloud and that cloud has a density [6]. Kuchero and Lavrovsky [10] invented electron cloud densitometry, the essence of which is that an electron beam, passing through an atom, receives information about the shapes of electron clouds. Below is a comprehensive presentation of this theory [13].

Consider two objects of quantum mechanics: a) an atom with inner and valence electrons and b) an external plane electron wave. The quantum mechanical objects have the properties of waves and particles at the same time. The objects are waves.

The basis of quantum mechanics is the statement that the wave function $\Psi(x,y,z)$, with coordinates x, y, z , describe the state of the system and the square modulus of this function determines the probability to find the system in the volume $dx dy dz$.

$$P(x,y,z)=|\Psi(x,y,z)|^2 dx dy dz. \quad (1)$$

The wave function of the electron beam \sqrt{j} is a plane wave, it is given by the current density and does not depend on the coordinates $\sqrt{j}(x,y,z) = \text{constant}$.

The wave function of the atomic electron is $\varphi(x,y,z)$ and the square module of this function determines the electron cloud density $\rho(x, y, z)$ in the volume $dx dy dz$.

$$\rho(x,y,z)=|\varphi(x, y, z)|^2 dx dy dz. \quad (2)$$

Let us find the electron cloud density $\rho(x,y,z)$ by taking advantage of the fact that the objects have the properties of particles. The objects are particles. The quantum mechanics particles obey the principle of superposition: the probability of meeting at a certain point $|\Psi(x,y,z)|^2 dx dy dz$ is equal to the product of the probabilities of each particle to get to this point.

$$P(x,y,z)=|\sqrt{j}|^2 \times |\varphi(x,y,z)|^2 \quad (3)$$

In this case, the following integral of Eq. (6) from z_{min} to z_{max} defines the probability $I(x,y)$ to find the electron at point x, y of the atomography.

$$J(x,y) = j \times \rho(x, y) \tag{4}$$

Thus, the plane wave amplitude $J(x,y)$ is proportional to the electron cloud density $\rho(x,y)$ or the thickness of the electron cloud of the atom at the point of the beam passage. The cloud changes the current not by absorption or amplification, but by spatial shift under the influence of quantum superposition. This is a purely quantum effect, it is absent both in optics and in electrodynamics.

The theory set out above is accurate and not approximated in any way.

Law 1. *Thus, the interaction of the electron beam with electron clouds under the influence of quantum superposition obeys the Kuchеров law: **the current passed by an electron cloud is proportional to the density of that cloud.***

That is, all atoms shift the plane electron wave in proportion to the density of the cloud density $\rho(x,y)$, and, as a result, create an atomographs.

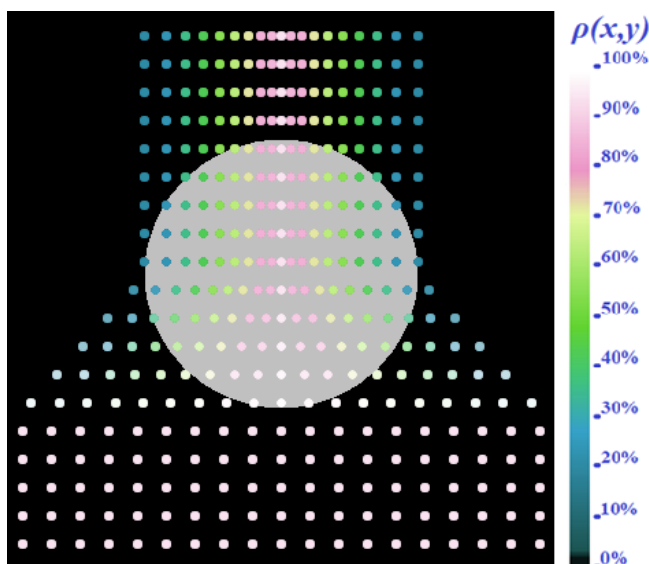


Fig. 2. The atom shifts the electron beam in proportion to its own density $\rho(x,y)$. The density scale is shown on the right.

Figure 2 shows the property of an electron cloud to shift the electron beam. The electron rays pass through the atom without absorption. However, under the influence of quantum superposition, the electron cloud shifted an electron beam without changing its speed and direction. On the periphery, where the electron cloud is absent, the rays completely disappear respectively. The intensity of the rays increases in the center, where the thickness of the electron cloud reaches a maximum. As a result, the atom begins to illuminate, depicting its internal construction.

2.3. Fundamental difference from the transmission

Particle size and structure have a great influence on the type of measurement methods used in nanoscale studies. Particles with sizes of the order of a nanometer can be visualized using a transmission electron microscope (TEM) [20]. For particles below 100 nanometers, a scanning

tunneling microscope (STM) can be used [3]. Even smaller particles can be examined using an atomic force microscope (AFM) [19].

Given the above, let's look at comparative characteristics of the picoscope with the transmission electron microscope (TEM).

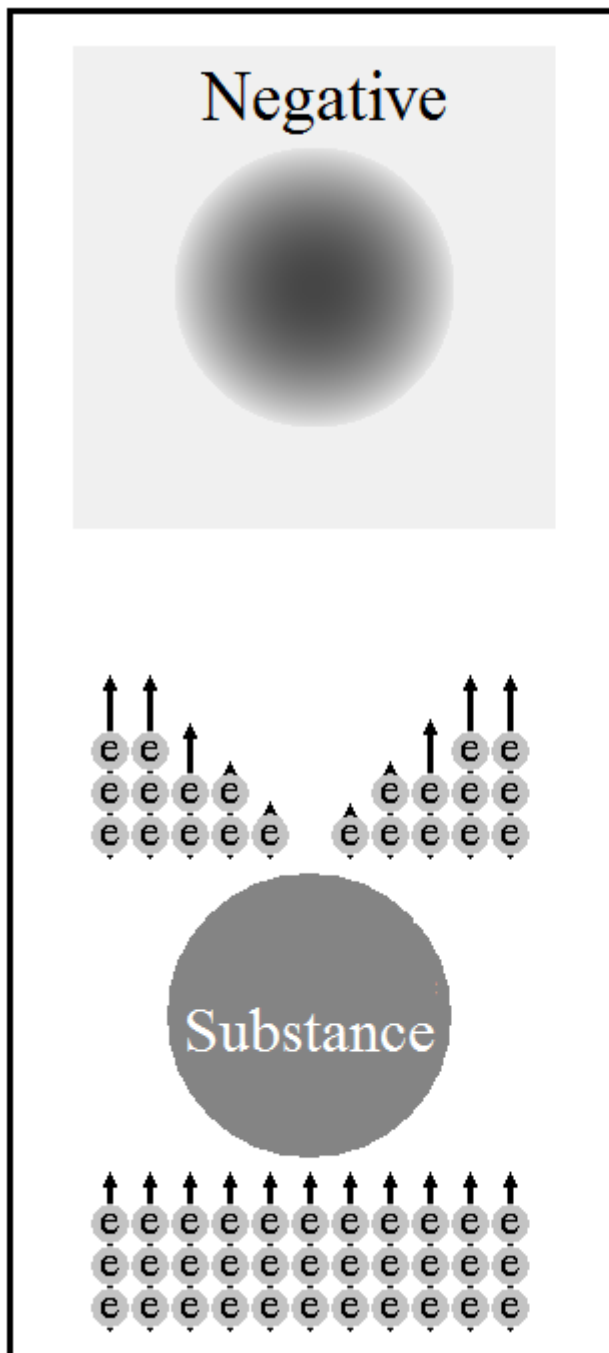


Fig. 3. Electrons are partially transmitted by substance and create a negative.

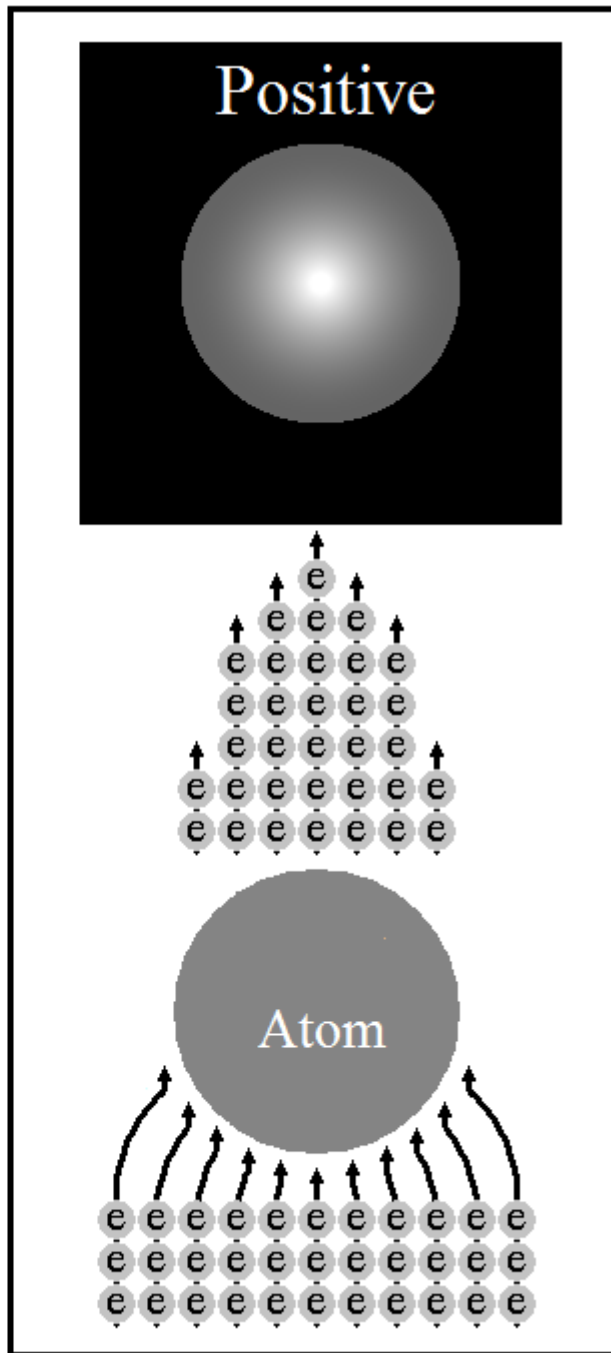


Fig. 4. Electrons are completely transmitted by any single atom, however, shift to its middle and create a positive.

Figure 4 shows the property of atoms to shift an electron beam in comparison with the property of a substance to absorb rays, Figure 3.

Figure 3 shows the properties of the electron beam to fix the structure of matter. Let the ray have 11 beams of 3 electrons each, that is, a total of 33 electrons. According to the property of matter to absorb electrons, their intensity increases with decreasing sample thickness. Figure 3 shows that only 20 electrons transmitted through the sample. Moreover, on the periphery, where there is no matter, all 3 electrons in each beam transmitted. As a result, the transmitted electrons create a negative of the test sample. So the transmission electron microscopes (TEM) make negative photo.

Figure 3 shows that matter (a large number of atoms) absorbs electrons, so the transmission electron microscope is not able to reflect the shape of a single atom.

Figure 4 shows the properties of the electron beam to fix the structure of a single atom by electron beam shifting effect. When the object under study is the size of an atom electron beams pass through the atom without absorption. However, they move towards the center of the atom without changing the direction and speed of movement. Figure 4 shows that all 33 electrons passed through the atom and shifted own trajectory. At the periphery, where there is no electron cloud, the rays have completely disappeared, having shifted their electrons to the center. The intensity of the rays increased in the center, where the maximum thickness of the atom. The result is a positive [10]. The atom lit up, accurately conveying its shape! So the picoscope makes positive atomographs.

Existing Transmission Electron Microscopes such as (HRTEM, JOL, JEM-2100, Japan) [15] or Philips 300 CM [16] have a resolution of about 100 picometers, while visualization of atomic-sized objects requires an instrument with a resolution of about 10 picometers.

The picoscope is a new tool for obtaining a atomography of atoms with a resolution of about 10 picometers. It was found by academicians O.P. Kucherov and I.E. Lavrovsky Patent of Ukraine [6, 9], we will describe the principle of its operation.

Next, we will demonstrate the limitless possibilities of picoscopy.

3. VISIBLE CARBON ATOM

The atomography shows a carbon atom with all six electrons.

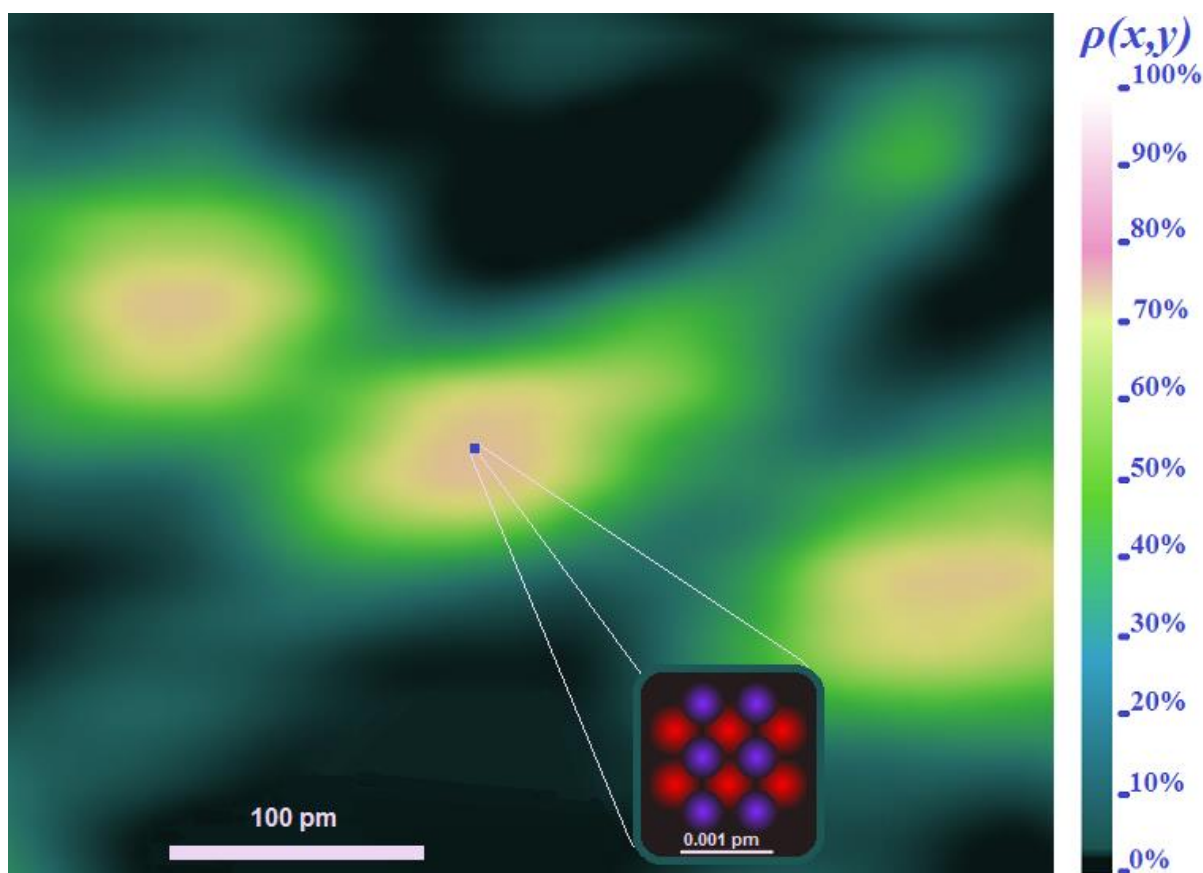


Fig. 5. Atomography of a carbon atom with six electrons: two pink inner electrons; two green covalent electrons and two blue active electrons.

The carbon atom has the sixth number in D.I. Mendeleev periodic table. Therefore, it has six protons, neutrons and electrons. Figure 5 shows all six electrons of the carbon atom: two pink inner electrons; two green covalent electrons and two blue active electrons. The protons and neutrons form the core, which has 0.001 pm in diameter. Red and blue balls show the core schematically.

Atomography 5 on the right shows the color scale of intensities, which, in accordance with the electron beam displacement law (10), conveys the density of electron clouds. A cloud with a maximum density of 100% is white. Space where there is no cloud, the intensity is zero, black.

Carbon atoms in crystalline graphite form layers by covalent chemical bonds sp^2 hybrids with have green constructions in the form of the infinity sign ∞ in accordance with the theory [13]. The blue active valence electrons that form the Van der Waals forces bound the layers.

A atomography of chemical bonds is shown in figure 3. The figure shows carbon atoms with their bonds in graphite: 1) atoms are pink; 2) covalent bonds - green; 3) Van der Waals forces - blue; 4) the space free from electron clouds is black.

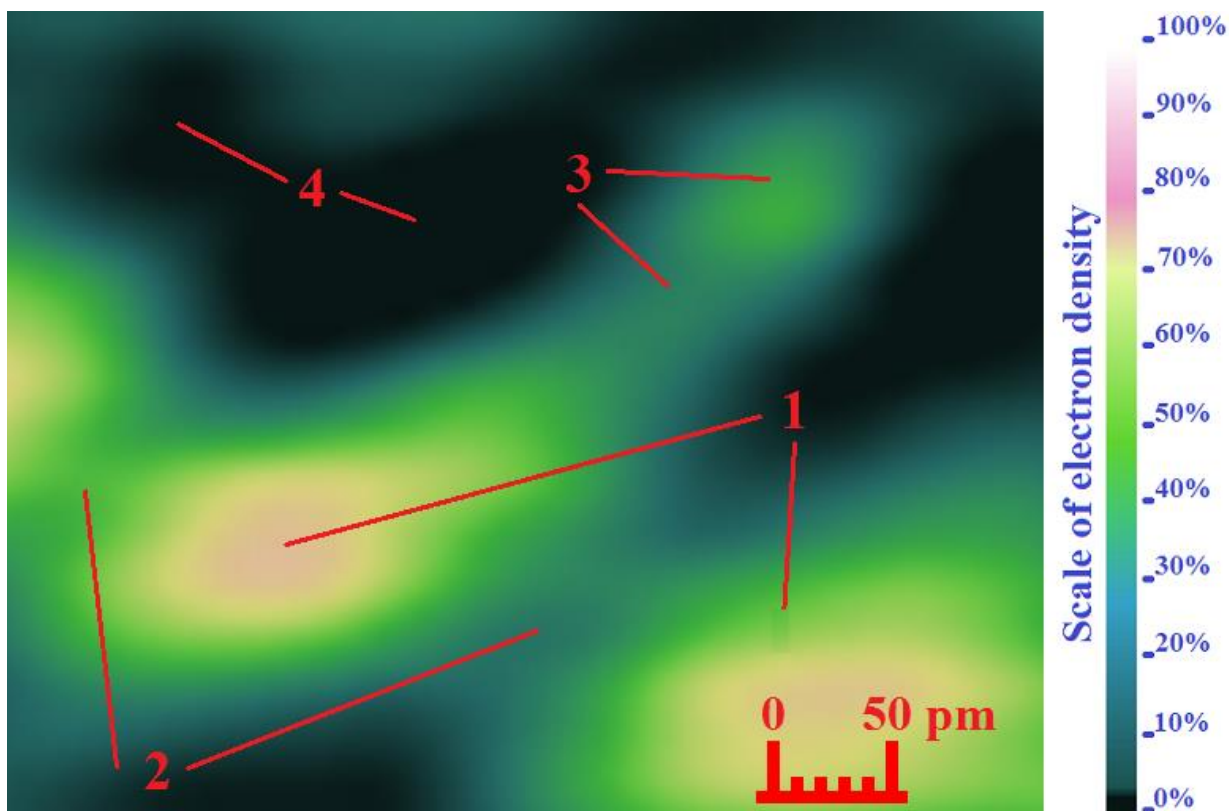


Fig. 6. Atomography of a carbon atom: 1) atom - pink; 2) covalent bonds - green; 3) Van der Waals forces - blue; 4) space free from electronic clouds – black [10].

Figure 6 shows carbon atoms (100% electron density) are bound by strong green covalent bonds (50% electron density).

Figure 6 shows the petals of blue - this is the connection of van der Waals. It turns out that this bond has its own shape, direction and electron density of 20%. Figure 6 shows numerous manifestations of it. The van der Waals bond is always tied to a particular atom, has an elongated shape, and never reaches another atom. This is not a bridge, this is a petal.

Note that the van der Waals forces are the forces of intermolecular (and interatomic) interaction with energy of 10–20 kJ/mol. These forces arise during the polarization of molecules and the formation of dipoles. They were discovered by Van der Waals in 1869. Thus, the visualization of chemical bonds confirmed the correctness of their description.

Connections of carbon atoms are possible in many variations. This is widely known as the strongest diamond and layered graphite. This is recently discovered graphene (Andre Geim and Konstantin Novoselov were awarded the 2010 Nobel Prize in Physics for their work on graphene), nanotube and fullerene (Kroto, Curl, and Smalley were awarded the 1996 Nobel Prize in Chemistry for their roles in the discovery of this class of molecules).

The picoscope allowed us to discover a number of new connections of carbon atoms. There are superdense substance rudenete [11], superthin gubanete [12] and non hybridized Musokhranov coke [16]. All three carbon allotropes were recently discovered with help of picoscope and can count on the Nobel Prize. Atomographies of all the listed allotropes of carbon will be shown below.

3.1. Graphite

Figure 7 shows a atomography of graphite (a crystalline form of carbon). Pink carbon atoms have their own shape and position. They are surrounded by green shells of covalent bonds that link carbon atoms into straight valence conduction bands.

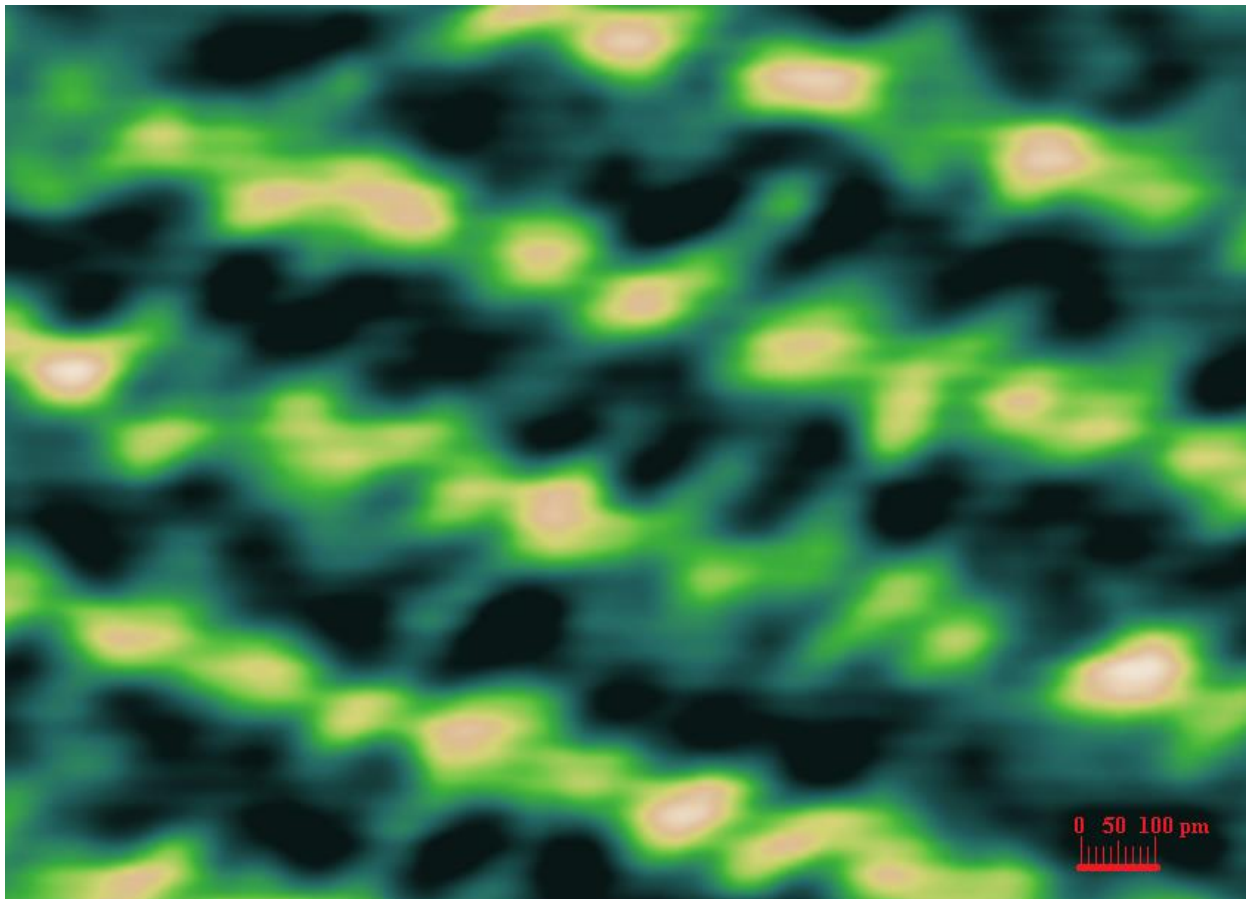


Fig. 7. Atomography of graphite with carbon atoms (pink), covalent bonds (green), weak van der Waals bonds (blue), and a zero-conductivity insulator layer (black).

The distance between the layers is 335 pm, and between the atoms - 128 pm, which corresponds to the data from the Encyclopedia.

The van der Waals system of weak bonds connects layers of graphite, which appear as elongated blue sleeves.

We have examined tens of thousands of van der Waals bonds and found that they are not abstract dipole interactions, but rather specific objects with their own characteristics. Therefore, in graphite, they have a light (blue) electron cloud in the form of a sleeve about 80 pm thick and about 160 pm long. The cloud is tilted at an angle of 66° to the graphite layer. They connect with one graphite layer, but do not reach the other. It is they that determine the semiconductor conductivity between the layers.

Figure 7 shows zones with different conductivities. Therefore, the conductor along the layer appears as bright green links. The elongated blue sleeves represent the semiconductor between the layers. The black zones of the insulator are clearly visible.

3.2. Graphene

The electron cloud densitometry was used to study atomographs of single-layer graphene.

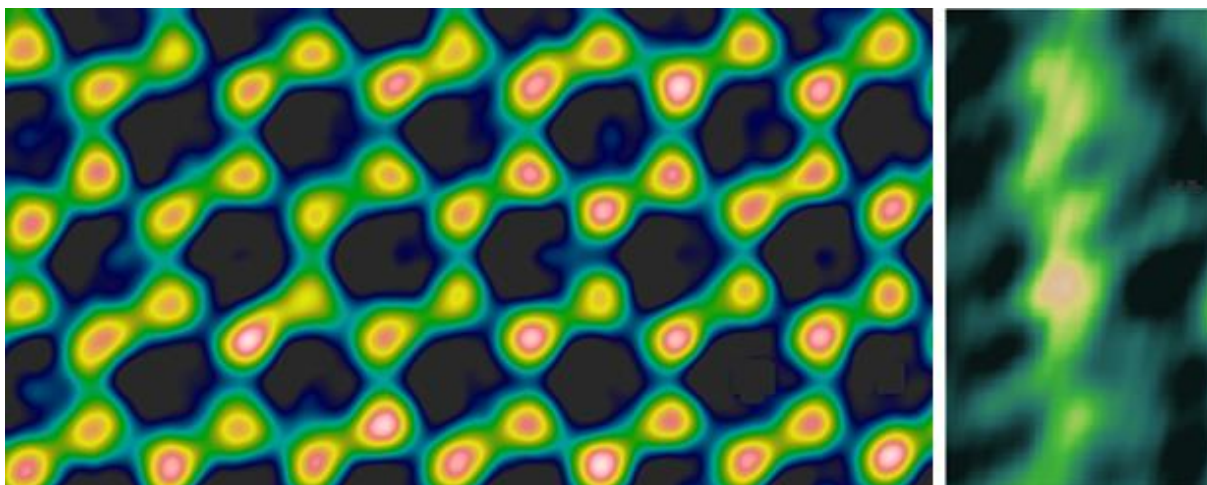


Fig.8. Atomographs of single-layer graphene, front view (left) and side view (right). The two inner electrons create a pink ball around the nucleus, the three sp^2 electrons create strong green hybrids; the one blue active electron is pulled to the side from each atom, as both photos show.

The atomographs (Fig. 8) show the hexagonal planar sp^2 hybrid constructions in the form of the infinity sign ∞ with three neighboring atoms. The active valence electron (blue) builds a negatively-charged shape due to its delocalization and occurs laterally from the graphene layer. This is seen in both photos.

Each carbon atom in graphene has three green sp^2 hybrids and one blue active electron.

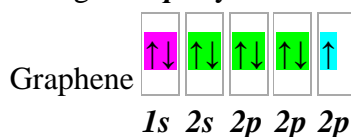


Fig.9. sp^2 hybrids in graphene.

Figure 10 shows the spatial 3d model of graphene. This and the next spatial 3d model are created using the molecular graphics program VMD [21]. Each carbon atom in the spatial 3d model is bonded by sp^2 hybrids to three adjacent atoms in a way that creates a hexagonal lattice. The active valence electron has an elongated negatively charged gray shape and goes away from the graphene layer.

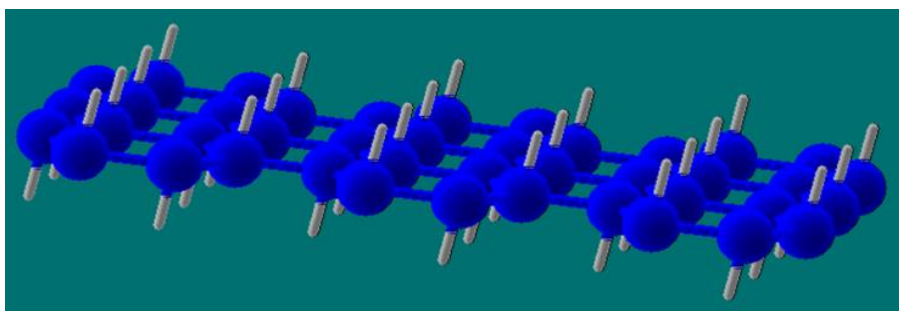


Fig. 10. Spatial 3d model of graphene. The layer of carbon atoms are connected by strong sp^2 hybrids and the gray active electrons are elongated out of the plane.

3.3. Diamond

Figure 11 shows the spatial 3d model of a crystal lattice of diamond with a tetrahedral structure. The carbon atoms have sp^3 hybrids inside and sp^2 hybrids with one active electron on a surface.

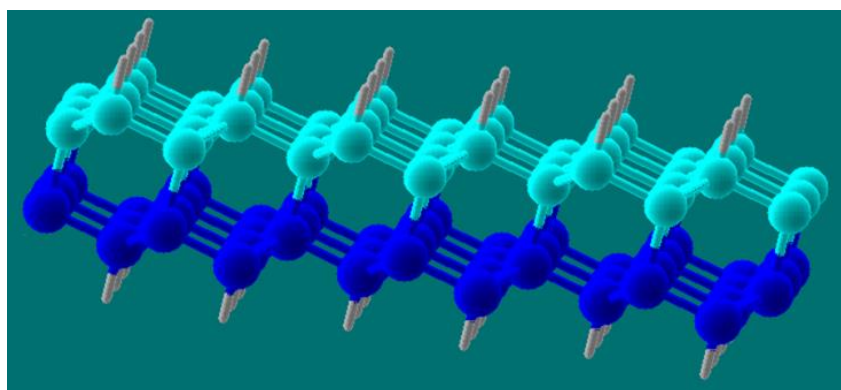


Fig. 11. Spatial 3d model of diamond. The carbon atoms are connected by sp^3 hybrids inside and by sp^2 hybrids outside. The gray active valence electrons at the diamond facets are pulled to the sides.

Carbon atoms are connected by strong sp^3 hybrids in the diamond inside. Each carbon atom has four sp^3 hybrids and has no active electrons:

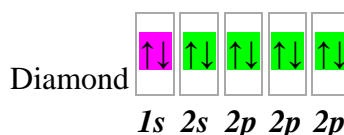


Fig. 12. Sp^3 hybrids in diamond.

However, on the diamond face, the fourth carbon atom is cut off; therefore, every fourth adjacent electron becomes active. Thus, each carbon atom has three sp^2 hybrids and one active electron.

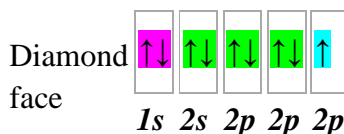


Fig.13. Sp^2 hybrids in diamond face.

Figure 14 shows the atomography of the diamond face with a tetrahedral structure. The carbon atoms have sp^2 hybrids of green. However, every third atom lies on the surface and has an active electron in it. This makes it brighter than other atoms, and the active electron amplifies its center to white.

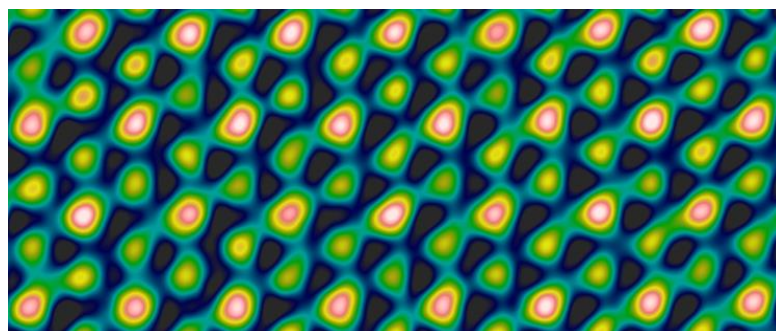


Fig. 14. Atomography of the diamond face. The carbon atoms are connected by green strong sp^2 hybrids. The active valence electrons at the diamond facet are white points [12].

3.4. Nanotubes

Figure 15 shows a atomography of carbon atoms forming two nested carbon nanotubes [8]. Each individual carbon atom is visible in the photo, so the inner nanotube has 6 carbon atoms, and the outer one has 12. In addition, the gap on the upper right is clearly visible on the outer nanotube. The distance between nanotubes is 120 picometers.

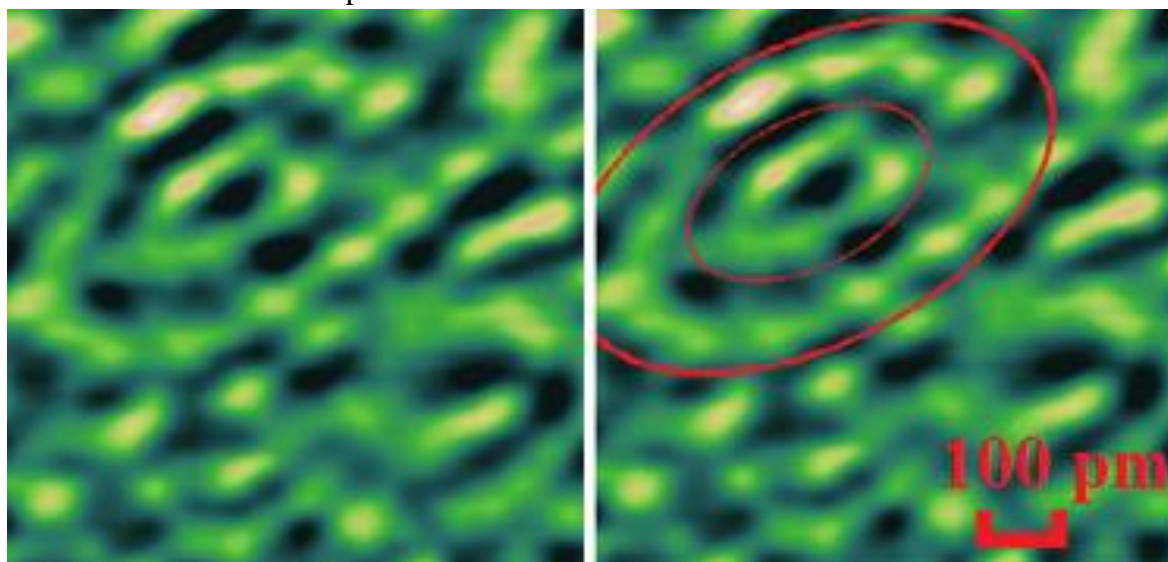


Fig. 15. Atomography of two nested nanotubes with an average distance of 120 pm [8].

Figure 15 shows the atomography of the atoms that make up the intersection of four embedded tubes with yellow and green conductive valence bands separated by black insulating layers.

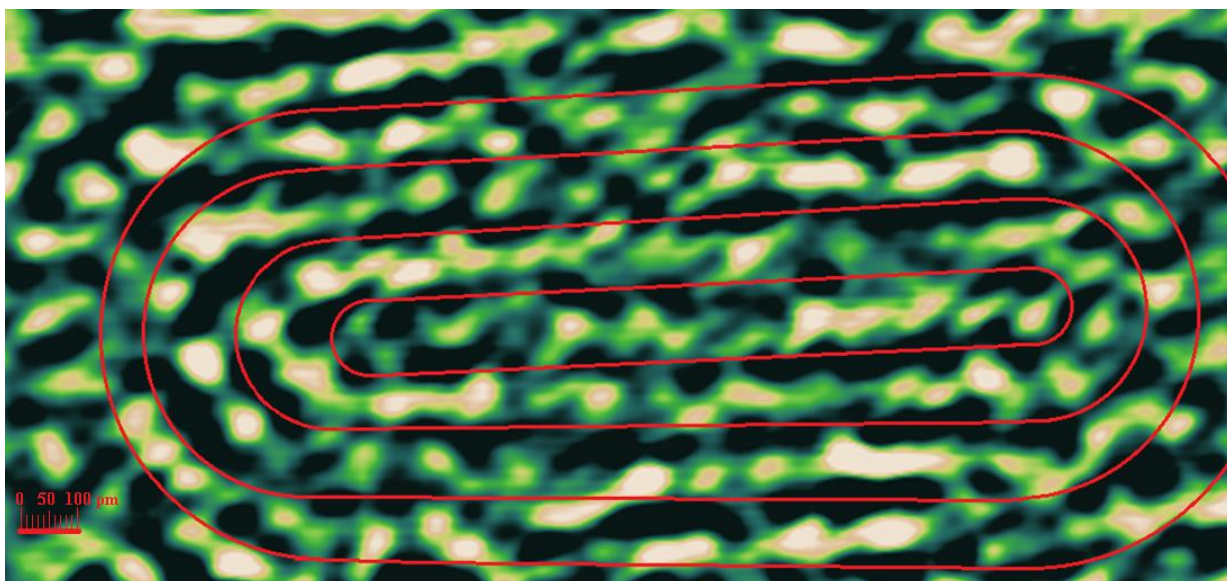


Fig. 16. A system of four nested carbon nanotubes.

Figure 16 shows an ultradense carbon nanotube which has yellow-green walls with an electron cloud density $\rho(x,y)$ of 60-90% indicating that the conductivity in the tube wall is higher than that of graphite. A black zone with zero conductivity is visible between the tubes, which is absent in graphite.

3.5. Rudenete

Many different structures of carbon are known and used in nanotechnology. These are diamond, graphite, graphene, fullerene, nanotubes, all of which were visualized using a picoscope.

In addition, a hitherto unknown formation of carbon was found [23]. This substance consists of two layers of graphite and has a density greater than that of diamond.

This is ultra-dense two-layer graphite. Its atoms are located at distances of 90-110 pm, which is much less than the distances between carbon atoms in diamond (128 pm).

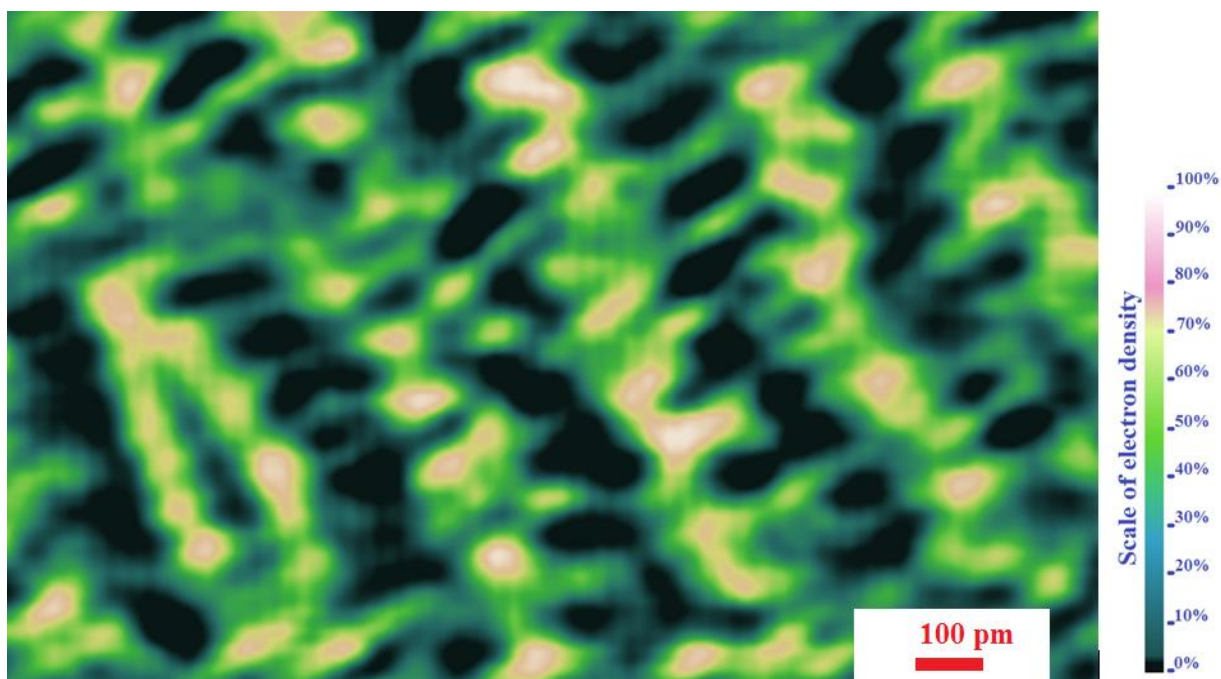


Fig. 17. Atomography of graphite layers (right) and ultra-dense two-layer allotropic structure of carbon (left) [23].

During spherical grinding, crystalline graphite undergoes a quasi-continuous structural transformation and passes into an amorphous state. These conditions lead to the creation of previously unknown densely local objects. This allowed the authors, together with Professor O.D. Rud to discover a new class of superdense carbon [23].

In this case, local internal self-stress occurs locally, which leads to an anomalous decrease in the distance between carbon atoms to 100 pm (molecular structure on the left in Figure 17, which is much less than the 128 pm distance typical for both graphite and diamond. The combined application of X-ray diffraction analysis, inverse Monte Carlo simulation, and the Voronoi diagram method, designed to simulate the atomic configurations of graphite, confirmed the existence of a superdense substance [22].

The discovery of the local allotropic structure of carbon was made together with scientists from the Institute of Metal Physics of the National Academy of Sciences of Ukraine and confirmed by a number of other indirect methods by researchers from several countries [4].

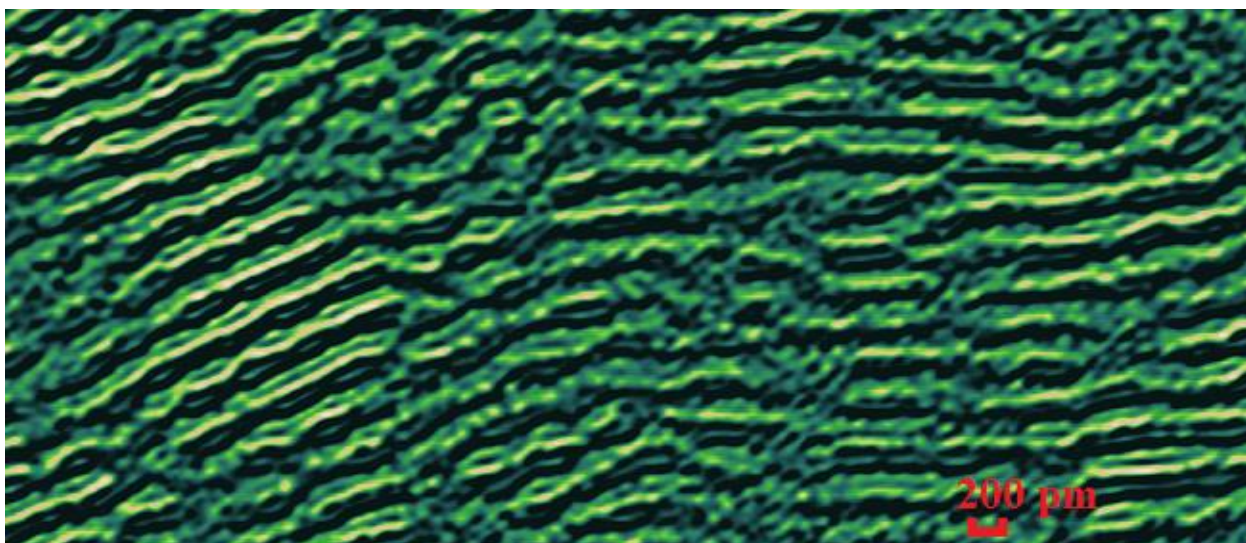


Fig. 18. Atomography of the material, where the content of ultra-dense two-layer graphite (rudenite) is increased.

Figure 18 shows a atomography of the material where the content of ultradense bilayer graphite (rudenite) is increased.

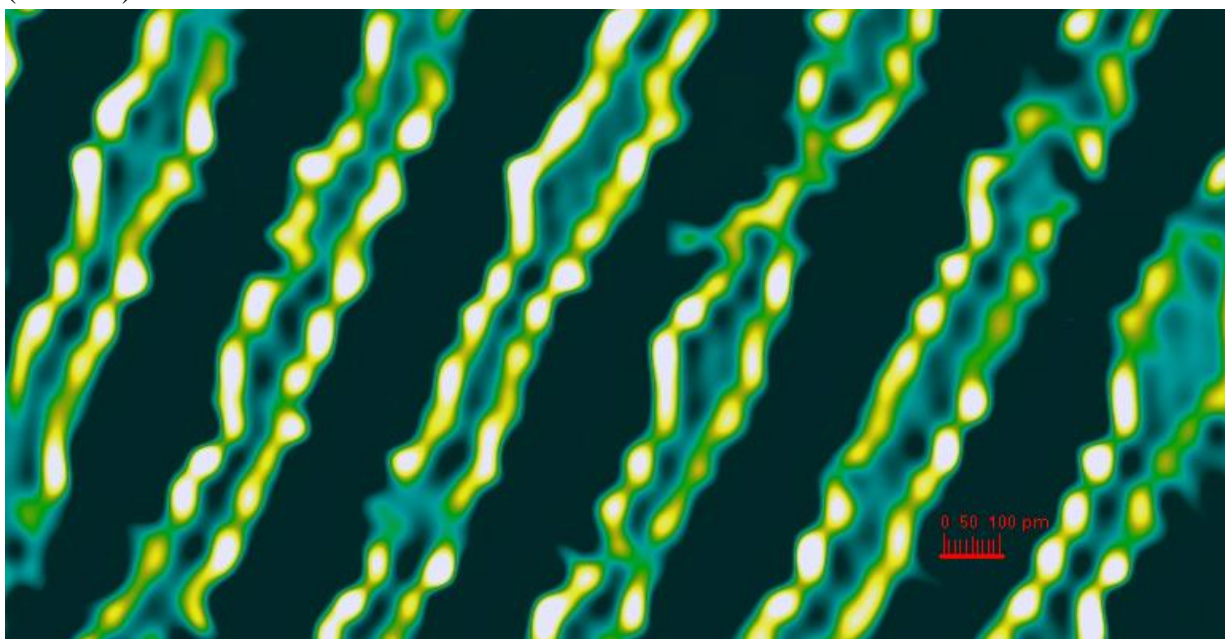


Fig. 19. Atomography of pure superdense two-layer graphite (rudenite).

Figure 19 shows a atomography of pure ultra-dense two-layer graphite(rudenite). It can be used for radiation shields and high capacity batteries.

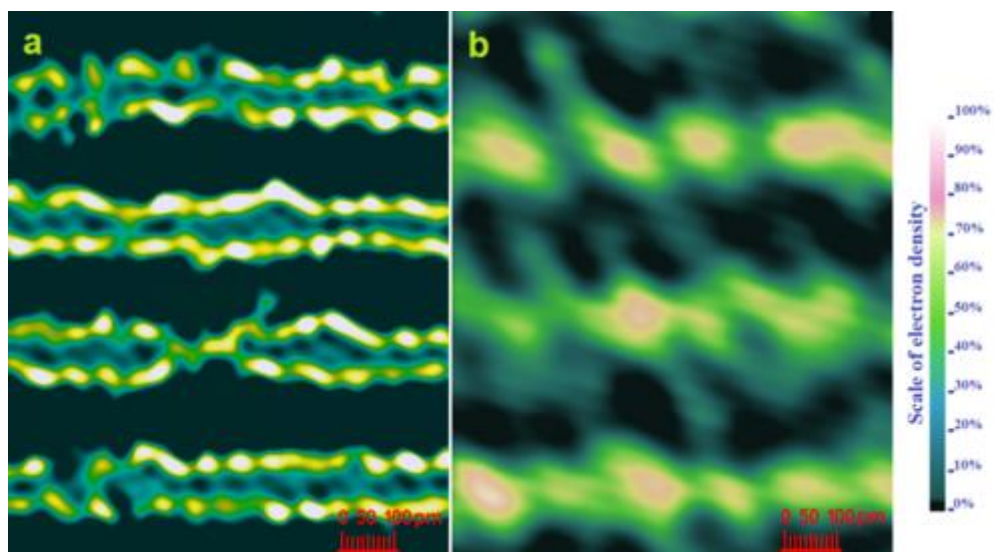


Fig. 20. Atomographs: a) rudenite - superdense allotropic form of carbon with a two-layer diamond-like structure, layers at a distance of 100 pm; b) graphite - layers at a distance of 340 pm. The scale of the electronic density of clouds is shown on the right.

Figure 20a shows a spatial ball-match 3D model of rudenite, top view. Two parallel layers of hexagonal structure are located at a distance of 100 pm. Each carbon atom forms four strong covalent sigma bonds of sp^3 hybridization: three in the plane and one between the planes. Due to the extremely small distance between layers, rudenite has a density 1.3 times greater than diamond. For example, the shortest distance between two adjacent carbon atoms in diamond is 154, in graphite - 140 pm. The ChemSpider is a free chemical database, from the Royal Society of Chemistry (RSC), it contains information on more than 100 million molecules from over 270 data sources. The uniqueness of rudenite is that none of the known molecules has such a small distance between atoms. Because of this, rudenite is a superdense [11] and ultrahard [4] material in the world.

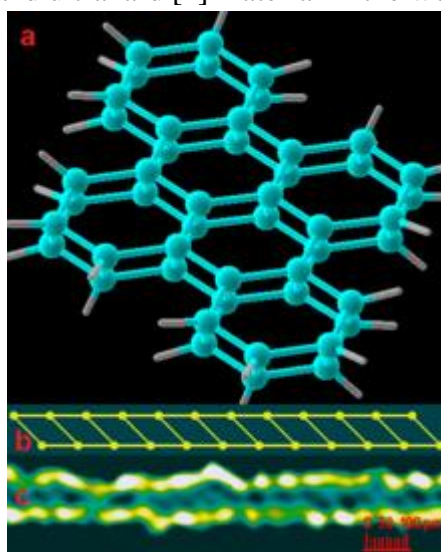


Fig. 21. Rudenite, a superdense film of two layers of flat hexagonal graphene. Spatial ball-match model of rudenite: a) 3D model, mountain view; b) side view; c) for comparison on the same scale with the model, a photo of electronic clouds of rudenite is shown from the side.

Calculations show that a capacitor made of ultra-dense bilayer graphite with a size of 1 cubic centimeter will have a capacitance of 8,000 farads. It can carry a charge of 100 kWh, which is enough for a Tesla car to travel 500 km.

3.6. Gubanete

This device allowed detecting a two-layer hexagonal diamond system that was previously unknown. This material is proposed to designate gubanite [12]. As the graphene layers converge, the upper graphene connect to the lower graphene active electrons to form a two-layer diamond gubanite.

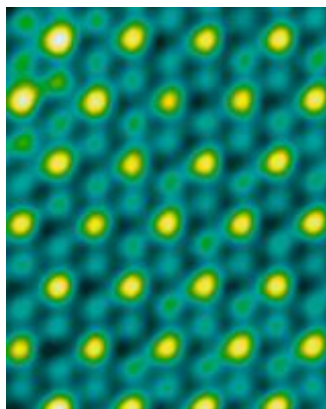


Fig. 22. Atomography of the gubanite. The carbon atoms are connected by green strong sp^2 hybrids. The active valence electrons at the gubanite facet are yellow points [12].

3.7. Active coal

Solid carbon exists in several allotropic forms: graphite, diamond, graphene, nanotubes, fullerenes, coke, vitreous carbon, and so on. In 1873, van der Waals discovered a force [24] that was later named after him. The van der Waals force includes attraction between atoms, molecules, and surfaces. They are active owing to polarization and weaker than covalent and ionic bonds. This force plays a major role in carbon allotropes. The Encyclopedia Britannica under the watchword "Structure of carbon allotropes" defines it as "the interlayer distance (337 pm) is sufficiently large to preclude localized bonding between the layers; the bonding between layers is probably by van der Waals interaction". A prominent quantum chemist Coulson entitled valence as "the distance between successive planes is 335 pm, a value so large that it can only arise from van der Waals forces". The Van der Waals force is present in the monolayer graphene [15]. The Van der Waals force is present in the activated carbon [17] embodied in both charcoal and coke.

The study shows that by electron cloud densitometry; there are active valence electrons in nature that builds negatively charged shape due to their delocalization. The active valence electrons create the van der Waals force, which, in particular, connects the layers of crystalline graphite [14].

Widespread activations of carbon are chemical [17], physical [1], or mechanical [21]. Amorphous carbon is synthesized by mechanical activation (MA) treatment of spectrally pure (99.99%) graphite in a Fritsch Pulverisette P6 ball mill in SiN vial and milling balls in argon gas atmosphere (400 RPM, the mass ratio of balls and a sample of 30:1, the energy density of 2.42 W/g). Specific energies (doses) transferred to the samples during grinding for 10 hrs were 87.1 kJ/g. The atomographs are obtained with a high-resolution electron microscope (JEOL JEM-2100F) by using the method in Ref. [10] with 10 pm resolution.

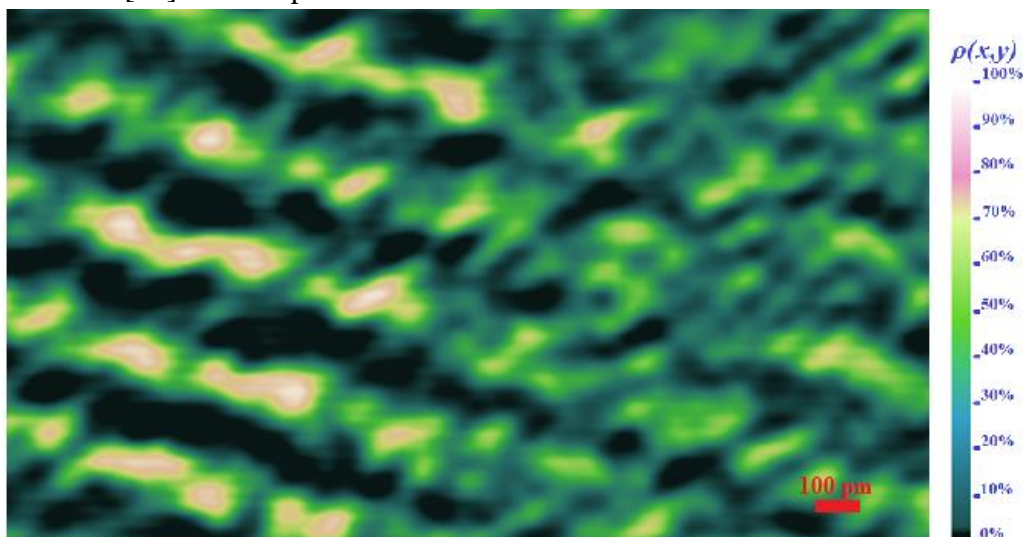


Fig. 23. Atomography of sp^2 hybridized carbon in crystalline graphite (left) and active coal without hybridization (right).[14]

The atomography (Fig. 23) shows the result of the activation. Carbon atoms in crystalline graphite (left) form layers by covalent chemical bonds sp^2 hybrids with have green constructions in the form of the infinity sign ∞ in accordance with the theory [13]. The blue active valence electrons that form the Van der Waals forces bound the layers.

4. VISIBLE ATOM TECHNOLOGY

The picoscope allowed us to discover a number of new sciences: Visible chemistry; Visible molecular physics; Visible resistance of materials; Visible physics of semiconductions; Visible microelectronic; Quantum dots visualization. Each of these new sciences can count on a Nobel Prize.

Here the word *visible* means direct visualization of individual atoms, molecules and chemical bonds. The atomographs below demonstrate the limitlessness of the possibilities of these sciences.

4.1. Visible chemistry.

The direct visualization of chemical bonds shows the existence of active valence electrons and two chemical bonds: the ion bonds and the covalent bonds.

Let's show them.

Visualisation of the ion bonds. By definition, in an ionic bond, one of the elements completely gives up an electron to another element. Everything is correct here. Based on this definition, in the model of C_5H_{12} pentane, presented in Figure 2c, there are no electron clouds around 12 proton nuclei. They have completely moved to the carbon atom figure 2b shows the pentane model. Conclusion: all models of water, alkalis, acids, organic substances that have an ionic bond with hydrogen must be redrawn and brought into line with reality.

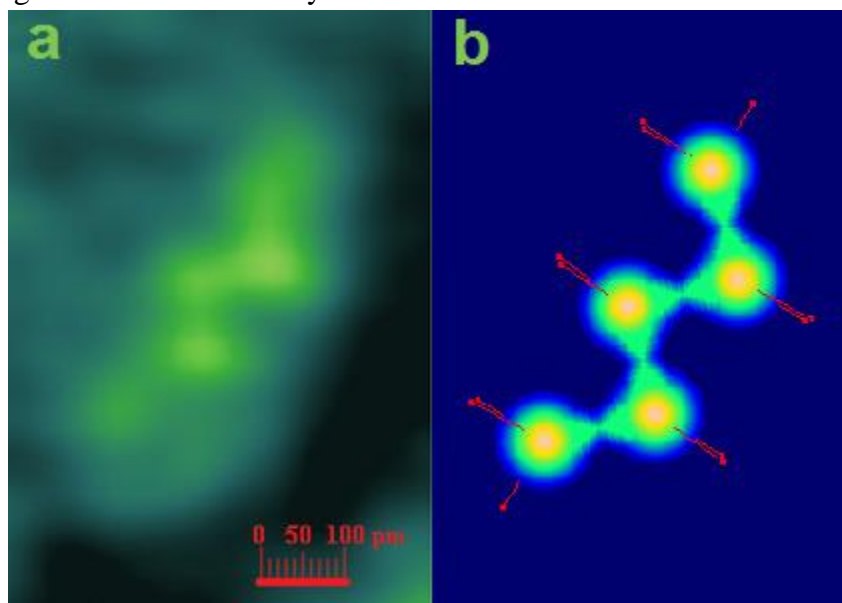


Fig. 24. Pentane C_5H_{12} with one molecule: a) atomography with a resolution of 10 pm [7]; b) a model of the pentane.

Figures 24 show a C_5H_{12} pentane molecule. Figure 24a shows the atomography of the electron clouds densities $\rho(x, y)$ of the molecule with resolution of 10 pm. The atomography shows all five electron clouds around the carbon atoms of the pentane molecule. According to the laws of quantum mechanics, the nucleus of hydrogen atoms devoid of electron clouds and, accordingly, hydrogen atoms are invisible in the atomography. The bond length between carbon atoms in the pentane molecule is 154 pm and the angle between them is 112° . Figure 24b shows a model of the C_5H_{12} pentane molecule, obtained as a result of X-ray diffraction analysis.

Every carbon atom in the pentane molecule has ten electrons, just like a neon noble gas.

The three inside carbon atoms have two strong sp hybrids of the covalent bonds (green) and two ion bonds from hydrogen atoms (red):

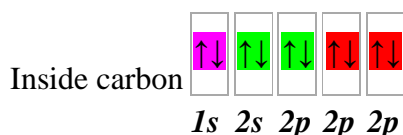


Fig. 25. Sp hybrids in inside carbon.

The two outside carbon atoms have one s hybrid of the covalent bond (green) and three ion bonds from hydrogen atoms (red):

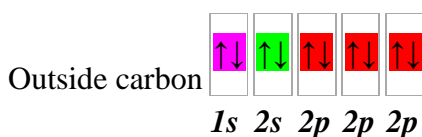


Fig. 26. S hybrid in outside carbon.

As a result, the picoscope makes it possible to visualize the atoms and molecules of various substances in real life.

Visualisation of the covalent bonds. Chemical bonds are the result of the interaction of electrons and atomic nuclei and are described by quantum mechanics. A single covalent chemical bond is created by a binding electron pair. In all current theories (the theory of valence bonds, the molecular orbital theory, the density functional theory, the density perturbation functional theory [19], the theory of repulsion of valence electron pairs, the Bohr model of chemical bonding [2]), the binding electron pair is located in the space between the atoms of the molecule.

In 1927, Heitler and London, [5] attempted to quantitatively mechanically calculate the ground steady state of the H₂ molecule. The success of this attempt became the basis for all further development of quantum chemistry.

The advent of visible chemistry makes it possible to create a general theory of the covalent bond of any identical atoms of the periodic table [13]. Usually the term "exact solution" in physics is understood as "accurate to the error of the experiment."

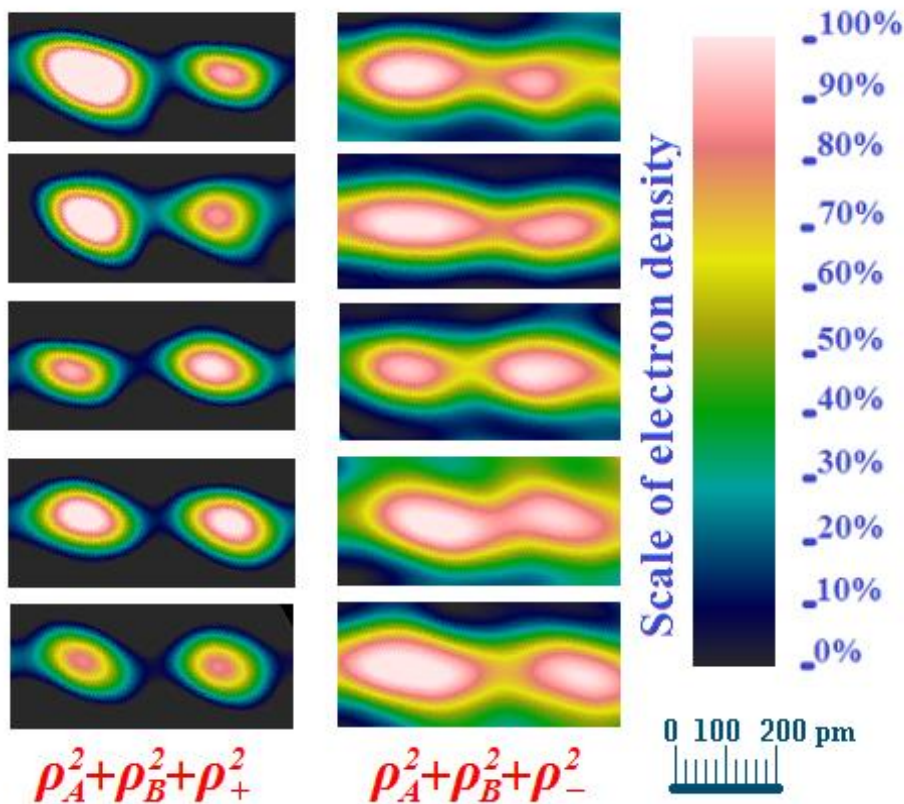


Fig. 27. Atomographs of electron clouds of silicon atoms symmetric $\rho_A(x,y)+\rho_B(x,y)+\rho_+(x,y)$ and anti-symmetric $\rho_A(x,y)+\rho_B(x,y)+\rho_-(x,y)$ covalent bonds. The electron clouds of the inner

electrons $\rho_A(x,y)$ and $\rho_B(x,y)$ are pink. Valence electrons are green - symmetric $\rho_+(x,y)$ on the left, anti-symmetric $\rho_-(x,y)$ - on the right [13].

Figure 27 shows atomographs of five electron clouds of silicon atoms symmetric $\rho_A(x,y)+\rho_B(x,y)+\rho_+(x,y)$ and anti-symmetric $\rho_A(x,y)+\rho_B(x,y)+\rho_-(x,y)$ covalent bonds. The electron clouds of the inner electrons $\rho_A(x,y)$ and $\rho_B(x,y)$ are pink. Valence electrons are green - symmetric $\rho_+(x,y)$ on the left, anti-symmetric $\rho_-(x,y)$ - on the right. The scale of electron cloud density and length scale are given next to it.

Visualization of active valence electrons. As firmly shown by electron cloud densitometry, there are the active valence electrons in nature that builds negatively charged shape due to their delocalization. The active valence electrons create the van der Waals force, which, in particular, connects the layers of crystalline graphite. The active valence electrons are visualized in active coal, graphite, graphene, and diamond. Each active valence electron builds a negatively charged long sleeve due to its delocalization.

Figure 28 shows a sharp change in chemical bonds as a result of activation (right). The green covalent chemical bonds sp^2 hybrids in the form of the infinity sign ∞ become blue active valence electrons and the crystalline structure is distorted. All active valence electrons have an elongated negatively-charged blue form and create amorphous chaos.

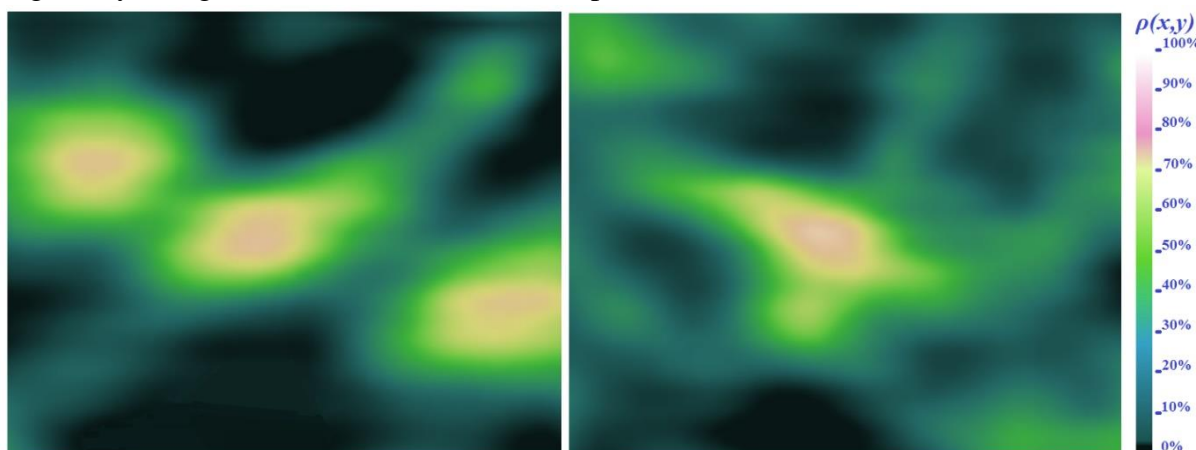


Fig. 28. Atomographs of a single carbon atom in a graphite crystal (left) and active coal (right). In each state, the atom has two inner pink electrons and four valence electrons. The difference is that the left atom has two green covalent and two blue active electrons, and the right atom has four blue active electrons [14].

Figure 28 left, shows a single carbon atom in crystalline graphite with six electrons. The two inner electrons have the shape of a pink ball. The two covalent bond electrons green create strong sp hybrids in the form of the infinity sign ∞ with two neighboring atoms. Each carbon atom in crystalline graphite is known to have three sp^2 hybrids, but Fig. 28 shows the edge of the crystal therefore the third hybrid atom is lacking. The two active valence electrons (blue) builds negatively charged shapes due to their delocalization and occur laterally from the graphite layer.

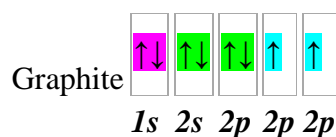


Fig. 29. Valence electrons in graphite layer.

The space between the layers is mostly black, signifying zero density of the electron clouds.

Figure 28 right, shows a single carbon atom in active coal with all its own six electrons. The two inner electrons have the shape of a pink ball. Four active valence electrons (blue) build negatively charged clouds elongated in different directions without hybridization.

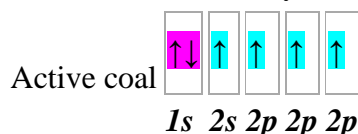


Fig. 30. In active coal all four active valence electrons exist without hybridization.

The active valence electrons create the van der Waals force and make coal active. The disappearance of covalent bonds during mechanical activation of graphite is confirmed by the decrease and expansion of the Raman vibrational bands sp^2 and sp^3 -hybridization [23]. In addition, the active valence electrons have opened up new materials with extraordinary technological properties. For example, cheap Musokhranov coke [16].

4.2. Visible molecular physics

Figure 30 shows the rotational motion of sapphire molecules. From left to right: "rings" turn into "horses" and then into "ellipses". The atomography shows how the "ellipses" turn into "rings" again.

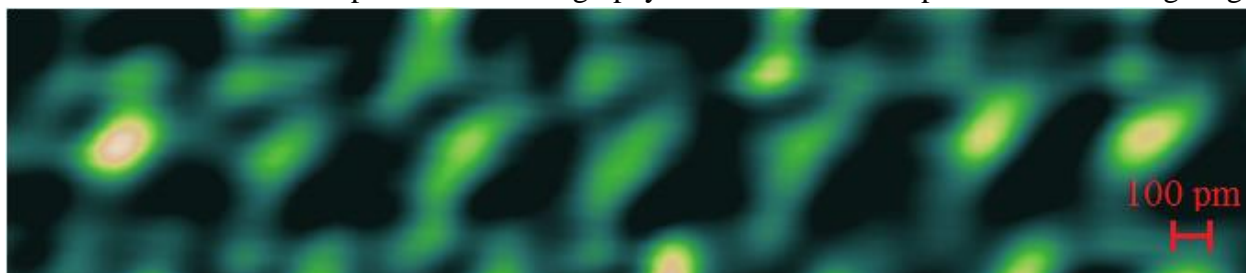


Fig. 31. Rotation of the sapphire molecule (A_2O_3). From left to right: "rings" turn into "horses" and further into "ellipses".

Such a change in the orientation of the sapphire molecule (A_2O_3) is associated with the influence of the silicon quantum dot, which is located above the crystal.

4.3. Visible resistance of materials

Figure 31 shows a atomography of graphite (a crystalline form of carbon). Yellow, purple, white carbon atoms have their own shape and position. The position of the atoms is determined with great accuracy as the maximum density of the electron cloud. The red pluses mark the calculation centers for the regular crystal lattice. The figure shows the shift of each atom from the theoretical center. This is a direct calculation of the deformation of the material.

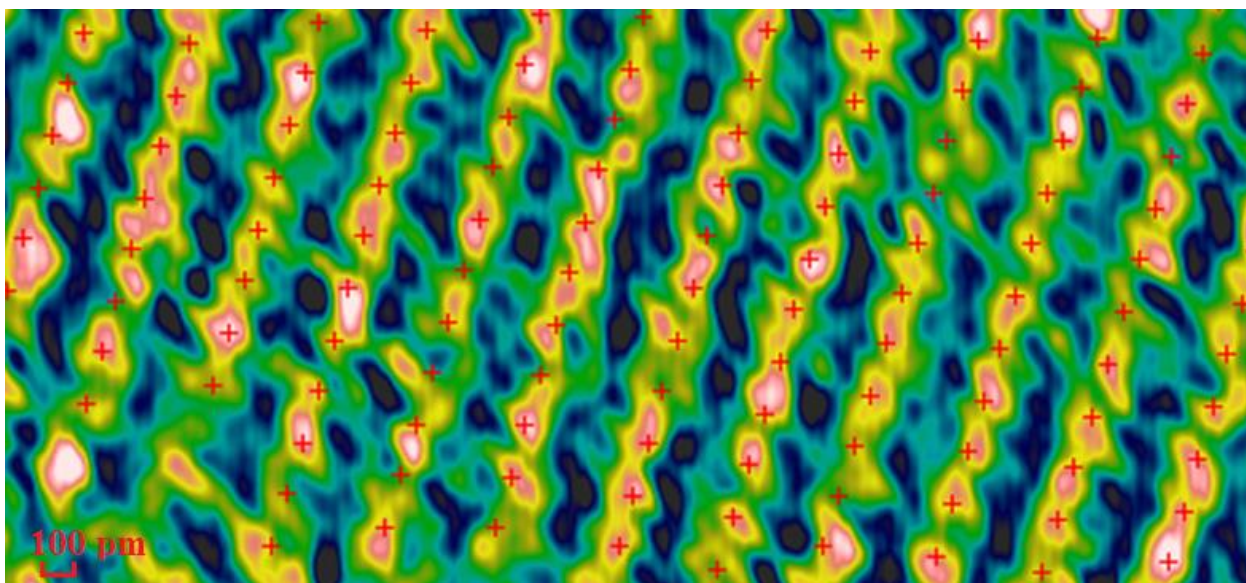


Fig. 32. Atomography of the crystal lattice of graphite. The crosses mark the centers of the crystal lattice.

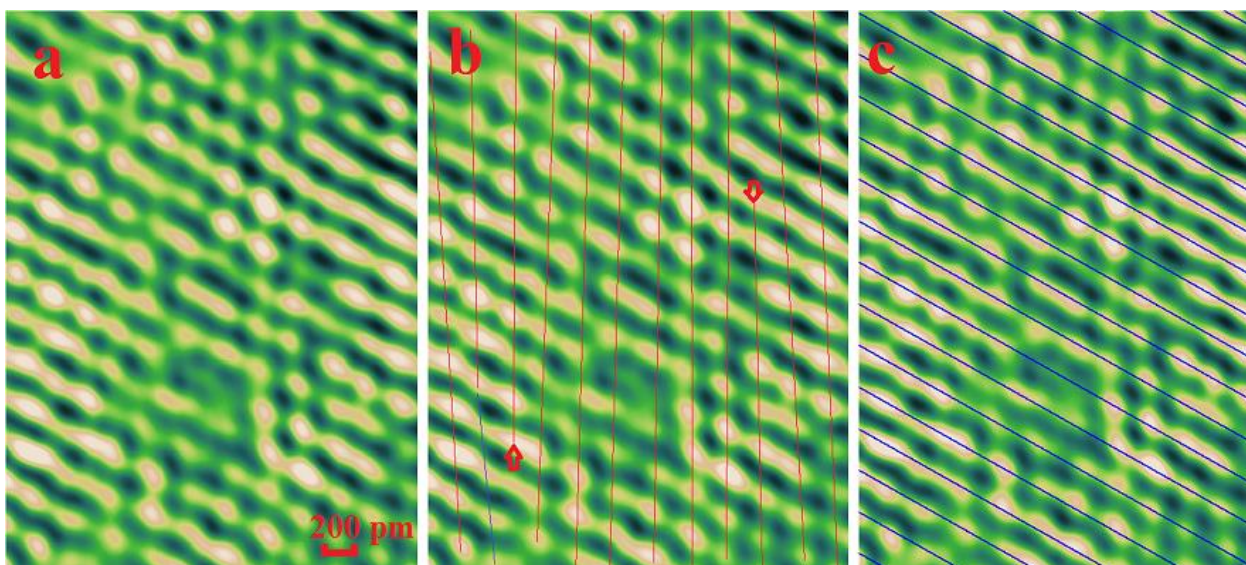


Fig. 33. Atomographs of atoms in a) crystal lattice; b) vertical layers have two collapses (We can see dislocations); c) horizontal layers are not damaged.

In figure 33b, the vertical layers in the crystal are drawn with red lines; it can be seen that 2 layers are interrupted, forming dislocations. Dislocations are indicated by arrows. Previously, the presence of dislocations could only be guessed from a sharp decrease in the strength of the material. The blue lines in figure 33c show the horizontal layers in the crystal. Horizontal layers are not damaged.

4.4. Visible physics of semiconductors

All electronics are built on two semiconductors - germanium and silicon. An important task is to study their properties, both separately and in a Ge/Si (100) solid solution. Ge/Si (100) heterostructures were obtained by molecular beam epitaxy (MBE). The sample was prepared in accordance with the

method described in [16]. The negative was obtained on a Philips 300 CM transmission electron microscope with an accelerating voltage of 300 kV and a resolution of 140 picometers [17]. After processing it according to method (12), a positive atomography of the electron clouds of Ge and Si atoms was obtained, in accordance with law (10), with a resolution of 10 pm (Fig. 34).

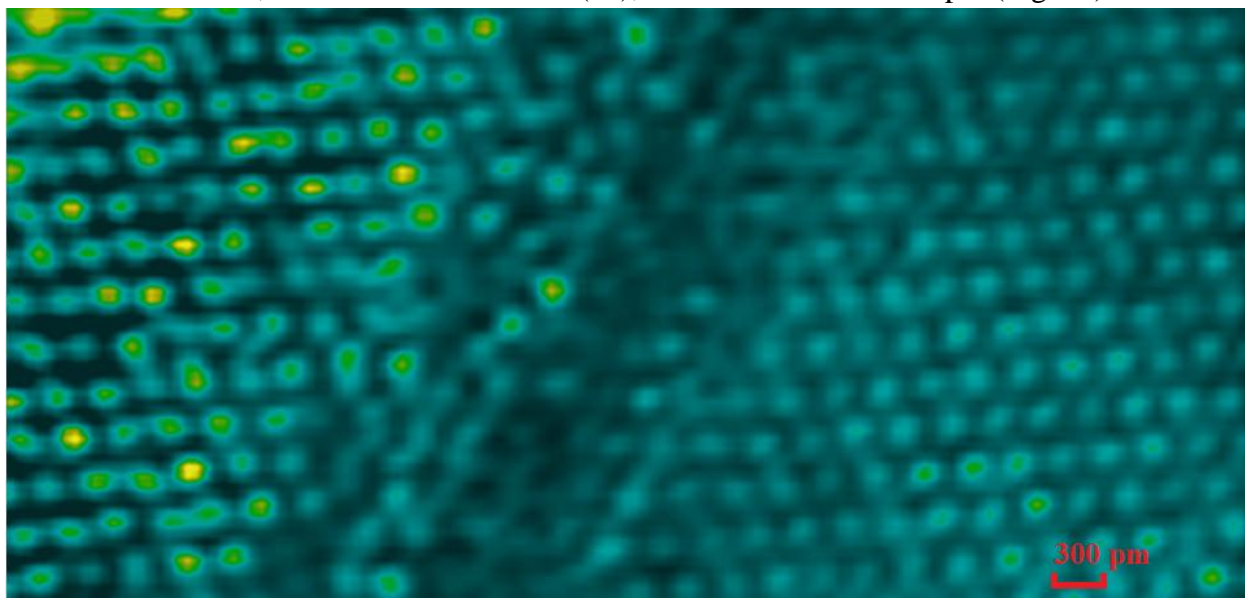


Fig. 34. Atomography of a Ge/Si (100) solid solution, left on a Si crystal, right. Ge atoms are yellow, Si atoms are blue.

Figure 34 shows a single-crystal silicon substrate (right), where the silicon atoms are blue. On the left, a Ge/Si (100) solid solution is visible, where blue silicon atoms alternate with yellow germanium atoms. In accordance with the electron cloud density scale blue corresponds to a density of 30%, and yellow to 70%. Given that there are 14 electrons in a silicon atom and 32 in a germanium atom, figure 34 correctly conveys the electron density of atoms. Thus, a method of direct measurement of atomic weight has been obtained.

In the Ge/Si (100) solid solution, we do not see quantum dots. Ge and Si atoms are mixed spontaneously without clusters.

If we draw lines along the layers of the lattice (Fig.35), we get an ideal single-phase single crystal, and there is no interface between the Si crystal and the Ge/Si (100) solid solution (green line).

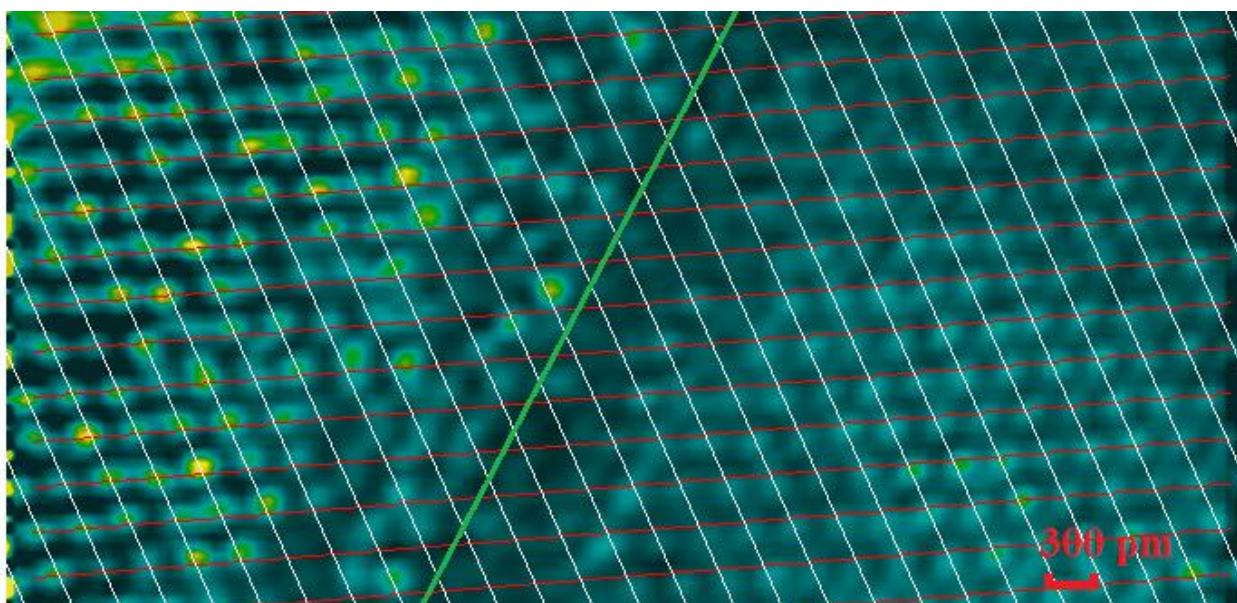


Fig. 35. The crystal lattice of silicon (right) and Ge/Si solid solution (left) form one ideal single crystal.

4.5. Visible microelectronic

Sapphire (Al_2O_3) is often used as a silicon crystal growth substrate in integrated circuits and solar power plants. The main problem in the production of integrated circuits is the quality control of the crystal. Using a picoscope allows you to accurately determine all violations of the crystal lattice and reject the workpiece with defects.

Figure 36 shows a tomography of a sapphire (Al_2O_3) crystal with a silicon quantum dot surrounded by amorphous silicon. The quantum dot which has a regular row of vertical layers of the crystal, but the horizontal layers are inclined at a large angle to the left of the red line and at a small angle to the right. That is, we see a previously unknown phenomenon of fused two quantum dots. That is, we observe the "quantum colon". Such a phenomenon cannot be detected by any known methods except picoscopy.

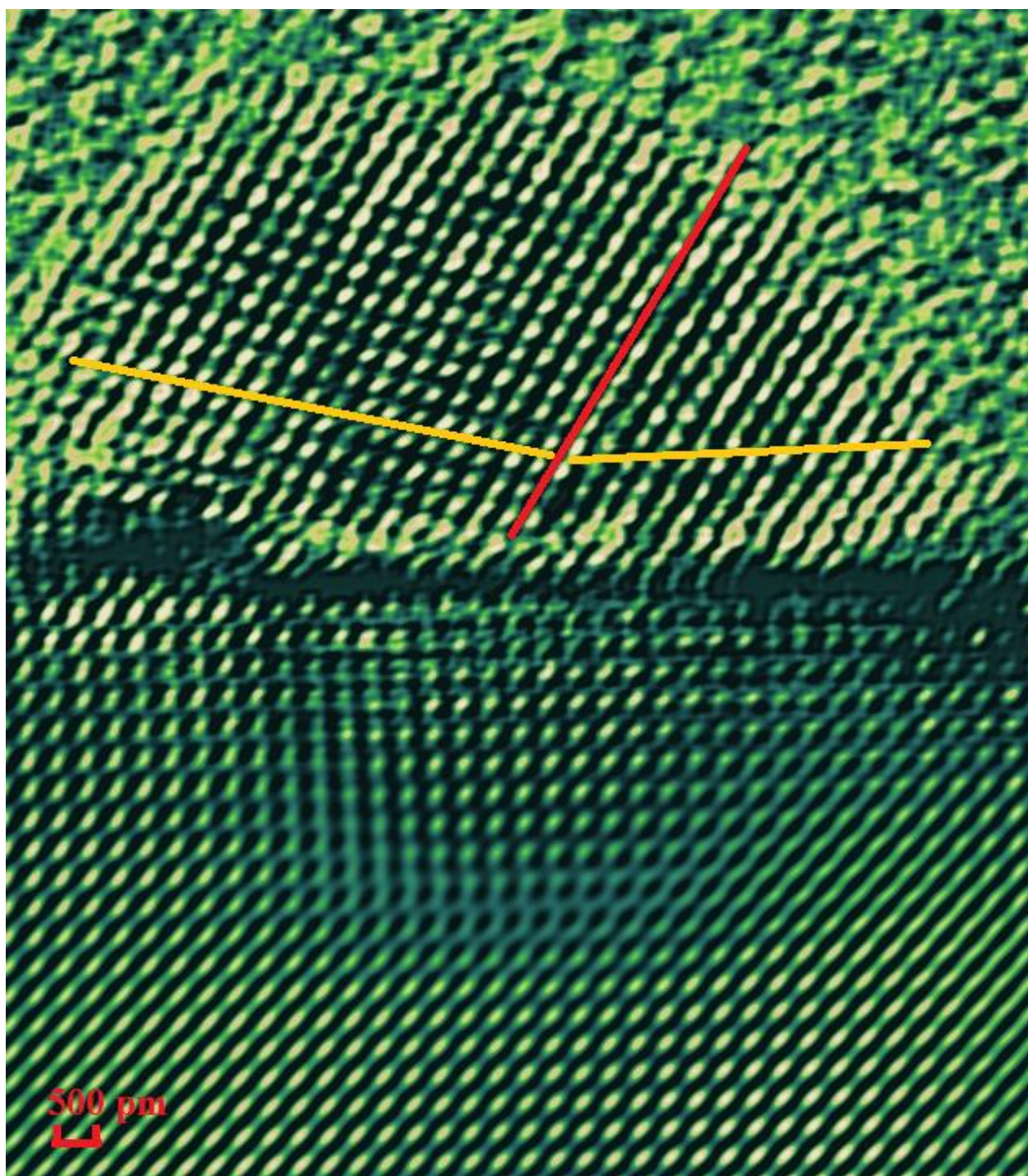


Fig. 36. Atomography of a silicon quantum dot surrounded by amorphous silicon on a sapphire (Al_2O_3) substrate

Figure 36 shows the phase change in the sapphire crystal near the quantum dot.

4.6. Quantum dots visualization

It so happened historically that humanity got acquainted with quantum dots much earlier than with any other nanoobjects. In the Middle Ages, metal nanoparticles were part of the paints used to make stained glass.

Quantum dots are used in field effect transistors, photocells, LEDs, laser diodes. The possibilities of using quantum dots as biomarkers for imaging in medicine and qubits for quantum computing are also being explored.

We present a study of hybrid quantum dots of zinc oxide with an average size of 5 nm on a graphene substrate, which increase the efficiency of power conversion in solar cells by 35%. The negative pimaged on a high resolution transmission electron microscope (HRTEM, JEOL, JEM-2100, Japan) [15]. After processing it according to the method (12), a positive atomography of the electron clouds of molecules was obtained by picoscopy with a resolution of 10 pm.

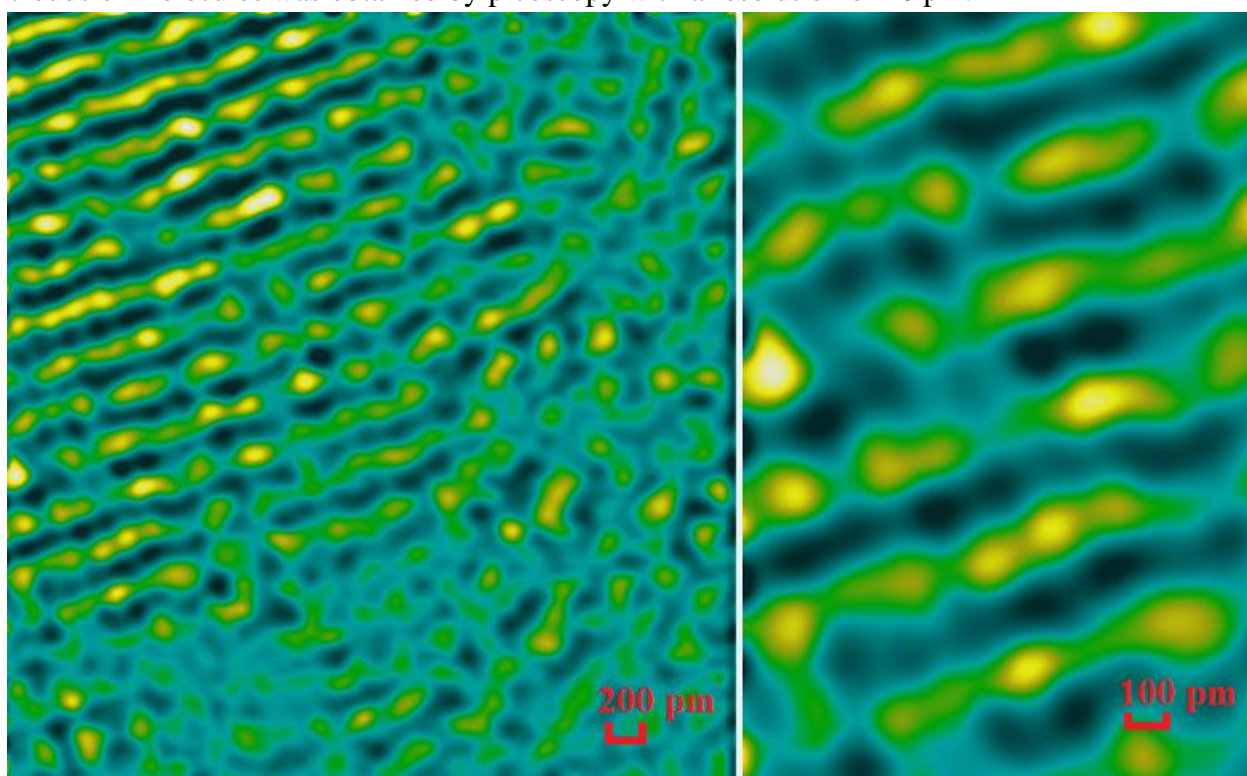


Fig. 37. A hybrid quantum dot of zinc oxide on a graphene substrate with a size of 5 nm. A complex spatial structure is visible, consisting of a valence band (yellow and green layers), semi-conduction bands (blue grid) and forbidden bands (black spots) [10].

Figure 37 shows ZnO molecules lined up in horizontal layers. A complex spatial structure is visible, consisting of a valence band (yellow and green layers), semi-conduction bands (blue grid) and forbidden bands (black bands). An enlarged view of this grid is shown on the right. The picoscope made it possible for the first time to visualize the spatial arrangement of the semiconductor bands and band gaps.

Conclusion

In his lectures on quantum mechanics, R.F. Feynman [6] said: "We know how ordinary objects behave, but small scale objects simply do not act in this way. Therefore, we must study them in some abstract or figurative manner, and not in connection with our direct experience."

The authors made the breakthrough in fundamental physics, namely the discovery of the unexpected natural phenomenon when the electron beam passing through the electron cloud shifts toward its center under the influence of quantum superposition. That is the electron beam shifting effect which leads to the fact that atoms and chemical bonds begin to illuminate in proportion to the electron clouds density. The atomography appeared as a result. It is the unique technique of direct visualization of atomic size objects: molecule, atoms and chemical bonds.

With the discovery of the atomography, the time for "abstract methods and figurative manners" has passed - now can we study the atomic size objects using our direct experience. This is a fundamental step towards understanding the logic of the behavior of the molecular world around us. The era when the teacher talks about molecules that he has never seen has ended and the era of unity with nature that consists of molecules.

Thus, with the advent of the atomography, schoolchilids and students were able to see the appearance of molecules as they are in nature. Chemistry, from a hypothetical subject, becomes natural and understandable, such as geometry, astronomy, biology.

Visualization of molecules greatly simplifies the teaching of natural sciences, expands the possibilities of existing ones and launches new ones.

The atomography opens the door to the world of molecules to create new technologies in materials science, crystallography, geology, microelectronics, biology, medicine and many other areas of science and technology. Direct visualization of atoms opens limitless horizons of possibilities for these new sciences.

References

1. Ahamed, K.R.; Handrasekaran, T.; Kumar, A.A. Characterization of activated carbon prepared from Albizialebeck by physical activation. *International Journal of Interdisciplinary Research and Innovations*. 2013, 1(1), 26–31.
2. W. Chen, V. Madhavan, T. Jamneala, M.F. Crommie, Scanning Tunneling Microscopy Observation of an Electronic Superlattice at the Surface of Clean Gold. *Phys Rev Lett* (1998) 80:1469. Doi:10.1103/PhysRevLett.80.1469.
3. Bohr, Niels (1913). "On the Constitution of Atoms and Molecules, Part III Systems containing several nuclei". *Philosophical Magazine*. 26 (155): 857–875. doi:10.1080/14786441308635031.
- 4 Gao, Yang; Cao, Tengfei; Cellini, Filippo; Berger, Claire; de Heer, Walter A.; Tosatti, Erio; Riedo, Elisa; Bongiorno, Angelo (2018). "Ultrahard carbon film from epitaxial two-layer graphene". *Nature Nanotechnology*. 13 (2): 133–138. arXiv:1801.00520. doi:10.1038/s41565-017-0023-9. PMID 29255290.
5. Heitler, W.& London, F. "Wechselwirkung neutraler Atome und homoopolare Bindung nach der Quantenmechanik" [Interaction of neutral atoms and homeopolar bonds according to quantum mechanics]. *Zeitschrift fur Physik*. 15-Humphrey, W.; Dalke, A.; Schulten, K. "VMD - Visible Molecular Dynamics" *J. Molec. Graphics*, 1996 14(1), 33–38.

6. Feynman Lectures on Physics, Quantum Mechanics. Palo Alto, London, 1961. – 325 p. (https://www.academia.edu/28997196/The_Feynman_Lectures_on_Physics_-_VOL3).
7. O.P. Kucherov, S.E. Lavrovsky, Picoscope, As an Instrument for Molecules Atomic Structure Study. Information technology and special security (2016), 73–81 (<http://science-ua.com/gallery/maketrn21.pdf#page=73>)
8. O.P. Kucherov, S.E. Lavrovsky, Electron Trajectory Shifting Effect. Abstract book. International research and practice conference: NANOTECHNOLOGY AND NANO-MATERIALS (NANO-2017) Chernivtsi. (<http://www.iop.kiev.ua/~nano2017/files/abstracts/Kucherov.pdf>)
9. Кучеров О. П., Лавровський С. Є. «Спосіб отримання зображення з субдифракційною роздільною здатністю та оптико-електронна система для його здійснення», Патент України № 115602 Від 27.02.2018р. (<https://uapatents.com/?search=115602&type=number>)
10. Kucherov, O.P.; Lavrovsky, S.E. Direct visualization of molecular structure by the electron beam shifting effect. Information technology and special security, 2018, 2(004), 12–41. (<http://science-ua.com/gallery/maketrn2.pdf#page=12>).
11. O. P. Kucherov & A. D. Rud (2018) Direct visualization of individual molecules in molecular crystals by electron cloud densitometry, Molecular Crystals and Liquid Crystals, 674: 1, 40-47, <https://DOI:10.1080/15421406.2019.1578510>.
12. Kucherov O., Rud A., Gubanov V., Biliy M. Spatial 3d Direct Visualization of Atoms, Molecules and Chemical Bonds // American Journal of Applied Chemistry. — 2020. — Т. 8, № 4. — С. 94—99. DOI: (<https://doi.org/10.11648/j.ajac.20200804.11>)
13. Kucherov, O. P. "Direct Visualization of Covalent Chemical Bonds in Crystalline Silicon". American Journal of Engineering Research (AJER). 2021, 10(6): 54–58. (<https://www.ajer.org/papers/Vol-10-issue-6/G10065458.pdf>)
14. Kucherov O. P. "Direct Visualization of Active Valence Electrons in Carbon Allotropes". American Journal of Engineering Research (AJER), vol. 11(02), 2022, pp. 19-25. (<https://www.ajer.org/papers/Vol-11-issue-2/D11021925.pdf>)
15. Lee, J.H.; al, Van der Waals force: a dominant factor for reactivity of graphene, Nano Lett. 2015, 15(1), 319–25. doi: 10.1021/nl5036012. Epub 2014 Dec 12.
16. Musokhranov B.A., SHARGE FOR PRODUCTION OF METALLURGICAL COKE (VARIANTS), Patent UA 92783 priority date 10 April 2007. (<https://base.uipv.org/searchin/search.php?action=viewdetails&IdClaim=152636>)
17. Nwankwo I.H. "Production and Characterization of Activated Carbon From Animal Bone." American Journal of Engineering Research (AJER), 2018, 7(7), 335–341
18. Omehe N. N., Otete I. "Ab initio study of the electronic band structure and phonon dispersion spectra of Silicon disulphide (SiP₂) and Silicon diarsenide (SiAs₂)." American Journal of Engineering Research (AJER), vol. 6, no. 12, 2017, pp. 439-447.
19. N. Pavlicek, B. Fleury, M. Neu, J. Niedenfuhr, C. Herranz-Lancho, M. Ruben, J. Repp, Atomic Force Microscopy Reveals Bistable Configurations of Diben-zo[a,h]thianthrene and their Interconversion Pathway. Phys Rev Lett (2012) 108:086101. Doi: 10.1103/PhysRevLett.108.246102.
20. A. Rosenauer, F.F. Krause, K. Muller, M. Schowalter, T. Mehrrens, Conventional Transmission Electron Microscopy Imaging beyond the Diffraction and Information Limits. Phys Rev Lett (2014) 113:096101. Doi: 10.1103/PhysRevLett.113.096101

21. A.D. Rud, I.M. Kiryan, A.M. Lakhnik, Topological characteristics of local atomic arrangements at crystalline-amorphous structural transition in graphite. *Materials Science. Mesoscale and Nanoscale Physics* (2014) (<http://arxiv.org/abs/1412.1982>).

22. A.D. Rud, N.E. Kornienko, I.M. Kiryan, A.N. Kirichenko, O.P. Kucherov, Local-Allotropic structures of carbon. The-sis "Carbon: the fundamental problems of science, materials science, technology". Troisk. (http://www.ruscarbon.com/tisncmdocs/2015/Carbon_Conference_2016-Thesis.pdf).

23. Rud, Alexander D.; Kornienko, Nikolay E.; Kirian, Inna M.; Kirichenko, Alexey N; Kucherov, O. P. (2018). "Local heteroallotropic structures of carbon". *Materials Today: Proceedings*. 5 (12): 26089–26095. doi:10.1016/j.matpr.2018.08.035.

24. Van der Waals J.D. (1873). *Over de continuïteit van den gas- en vloeistofoestand (On the Continuity of the Gaseous and Liquid States)* (doctoral dissertation). Universiteit Leiden.

РЕЦЕНЗІЇ ТА ІНФОРМАЦІЙНІ ПОВІДОМЛЕННЯ

ПРАВИЛА ДЛЯ АВТОРІВ

У науковому журналі «інформаційні технології та спеціальна безпека» друкуються статті, які відповідають профілю журналу і мають наукове та практичне значення. Редколегія просить не надсилати матеріали, раніше надруковані, чи такі, що готуються до друку в інших виданнях. Тексти статей та всі матеріали до них повинні бути ретельно відредаговані, перевірені та підписані авторами.

Надсилаючи статтю до редакції, просимо дотримуватись наступних правил

1. Рукопис надсилається в двох екземплярах, надрукований через 1,5 інтервали шрифтом Times 12 пунктів, набраний у редакторі Word-2003 та в електронному вигляді.

2. Розмір статті разом із рисунками та списком літератури не повинен перевищувати 10–12 сторінок і 5-ти рисунків. Викладення повинно бути чітким, стислим, без довгих вступів, відступів і повторів, а також без дублювання в тексті даних таблиць, рисунків і підписів до них. Реферат і розділ «Висновки», якщо він є, не повинні дублювати один одного. Обсяг реферату — не більше 1000 знаків. На першій сторінці статті має бути зазначено індекс УДК.

3. Назву статті, ініціали та прізвища авторів, повну назву установи та її адресу, де працюють автори, а також текст реферату та ключові слова друкують мовою статті. Окремим файлом подають ті ж самі дані (крім адреси та назви установи) іншими двома мовами (англ., укр./рос.)

4. Рисунки (діаграми, графіки, фотографії тощо) потрібно подавати на окремих сторінках на білому папері, чітко віддруковані (чорно-біле зображення) і підписані на зворотній стороні листа. Рисунки необхідно подавати кожний окремим файлом. Бажана ширина рисунків — 75мм або 150 мм. Надписи на рисунках слід, по можливості, замінити літерними позначками, а криві позначити цифрами, які роз'яснюються в підписах до рисунків або в тексті. Мінімальний розмір надписів на рисунках — 10 пунктів. Не бажано наводити у вигляді рисунків дані, які можна представити в тексті чи в таблиці. Місце рисунків указується на лівому полі рукопису. Підписи до рисунків бажано давати окремим файлом.

5. Таблиці повинні мати номер і назву. Кожний рисунок і таблиця — відповідні посилання в тексті. Скорочення слів у тексті, таблицях і на рисунках не дозволяються.

6. Формули повинні бути набрані у редакторі Microsoft Equation шрифтом 12 пунктів (Italic). Грецькі літери слід підкреслити і на полях написати їхню назву. Розмітити олівцем великі та малі літери, які мають однакове написання (\underline{C} , \bar{c} , \underline{K} , \bar{k} тощо). Літери й знаки, які важко відрізнити, слід пояснити на полях олівцем: J (йот), I (і), 1 (одиниця), l (ель), 0 (нуль), O (літера) тощо.

7. Стаття повинна мати список джерел, що цитується. Список оформлюється згідно ДСТУ ГОСТ 7.1.2006 «Система стандартів з інформації, бібліотечної та видавничої справи. Бібліографічний запис. Бібліографічний опис. Загальні вимоги та правила складання. З прикладами складання бібліографічного опису можна ознайомитися в Бюлетені ВАК України № 5 за 2009 рік. Посилання на літературні джерела в тексті статті слід давати в квадратних

дужках у вигляді порядкової цифри, надрукованої у рядок.

8. На окремому аркуші подаються відомості про всіх авторів: прізвище, ім'я та по-батькові (повністю), вказується вчена ступінь та звання, посада, повна назва установи, а також домашня та службова адреси із зазначенням індексу, номер телефону кожного автора та e-mail (за бажанням авторів).

Рукописи, що не відповідають цим вимогам, розглядатися не будуть.